

Interactions between main-channels and tributary alluvial fans: channel adjustments and sediment-signal propagation

Sara Savi¹, Stefanie ~~Tofelde~~^{2,3}~~Tofelde~~^{1,2}, Andrew D. ~~Wickert~~⁴~~Wickert~~³, Aaron ~~Bufe~~³~~Bufe~~², Taylor F. Schildgen^{1,3,2}, and Manfred R. Strecker¹

¹Institut für Geowissenschaften, Universität Potsdam, 14476 Potsdam, Germany

~~²Institut für Umweltwissenschaften und Geographie, Universität Potsdam, 14476 Potsdam, Germany~~

~~³Helmholtz²Helmholtz Zentrum Potsdam, GeoForschungsZentrum (GFZ) Potsdam, 14473 Potsdam, Germany~~

~~⁴Department³Department of Earth Sciences and Saint Anthony Falls Laboratory, University of Minnesota, Minneapolis, MN 55455, USA~~

Corresponding Author: Sara Savi (savi@geo.uni-potsdam.de)

Abstract

Climate and tectonics impact water and sediment fluxes to fluvial systems. These boundary conditions set river form and can be recorded by fluvial deposits. Reconstructions of boundary conditions from these deposits, however, is complicated by complex channel-network interactions and associated sediment storage and release through the fluvial system. To address this challenge, we used a physical experiment to study the interplay between a main channel and a tributary under different forcing conditions. In particular, we investigated the impact of a single tributary junction, where sediment supply from the tributary can produce an alluvial fan, on channel geometries and associated sediment-transfer dynamics. We found that the presence of an alluvial fan may either promote or prevent sediment to be moved within the fluvial system,

27 creating different coupling conditions. ~~A prograding alluvial fan, for example, has the potential~~
28 ~~to disrupt the sedimentary signal propagating downstream through the confluence zone.~~ By
29 ~~analyzing~~ analysing different environmental scenarios, our results ~~indicate~~ reveal the contribution
30 of ~~the two sub-systems both the main channel and the tributary~~ to fluvial deposits, ~~both~~ upstream
31 and downstream of the tributary junction, ~~which may be diagnostic of a perturbation affecting~~
32 ~~the tributary or the main channel only.~~ We summarize all findings in a new conceptual
33 framework that illustrates the possible interactions between tributary alluvial fans and a main
34 channel under different environmental conditions. This framework provides a better
35 understanding of the composition and architecture of fluvial sedimentary deposits found at
36 confluence zones, which ~~is essential for a correct~~ can facilitate the reconstruction of the climatic
37 or tectonic history of a basin.

38

39 1. Introduction

40 The geometry of channels and the downstream transport of sediment and water in rivers are
41 determined by climatic and tectonic boundary conditions (Allen, 2008, and references therein).
42 Fluvial deposits and landforms such as conglomeratic fill terraces or alluvial fans may record
43 phases of aggradation and erosion that are linked to changes in sediment or water discharge, and
44 thus provide important archives of past environmental conditions (Armitage et al., 2011;
45 Castelltort and Van Den Driessche, 2003; Densmore et al., 2007; Mather et al., 2017; Rohais et
46 al., 2012; Tofelde et al., 2017). Tributaries are an important component of fluvial networks, but
47 their contribution to the sediment supply of a river channel can vary substantially (Bull, 1964;
48 Hooke, 1967; Lane 1955; Leopold and Maddock, 1953; Mackin, 1948; Miller, 1958). Their
49 impact on the receiving river (referred to as *main channel* hereafter) may not be captured by
50 numerical models of alluvial channels, as most models either parameterize the impacts of
51 tributaries into simple relationships between drainage-basin area and river discharge (Whipple
52 and Tucker, 2002; Wickert and Schildgen, 2019), or treat the main channel as a single channel
53 with no lateral input (e.g., Simpson and Castelltort, 2012). Extensive studies on river confluences
54 (e.g., Rice et al., 2008 and references therein) mainly focus on (1) hydraulic parameters of the
55 water flow dynamics at the junction (Best 1986, 1988), which are relevant for management of

56 infrastructure (e.g., bridges), and (2) morphological changes of the main channel bed, which are
57 relevant for sedimentological studies and riverine habitats (Benda et al., 2004a; Best 1986; Best
58 and Rhoads, 2008). Geomorphological changes (i.e., channel slope, width, or grain-size
59 distribution) have been studied in steady-state conditions only (Ferguson et al., 2006; Ferguson
60 and Hoey, 2008), and with no focus on fluvial deposits related to the interactions between
61 tributaries and the main channel. In source-to-sink studies an understanding of these processes,
62 however, is relevant for the reconstruction of the climatic or tectonic history of a certain basin.

63 By modulating the sediment supplied to the main channel, tributaries may influence the
64 distribution of sediment within the fluvial system, ~~the duration of sediment transport from source~~
65 ~~areas to depositional basins (Simpson and Castellort, 2012)~~, and the origin and amount of
66 sediment stored within fluvial deposits ~~and~~ at confluence zones. Additionally, complex
67 feedbacks between tributaries and main channels (e.g., Schumm, 1973; Schumm and Parker,
68 1973) may enhance or reduce the effects of external forcing on the fluvial system, thus
69 complicating attempts to reconstruct past environmental changes from these sedimentary
70 deposits.

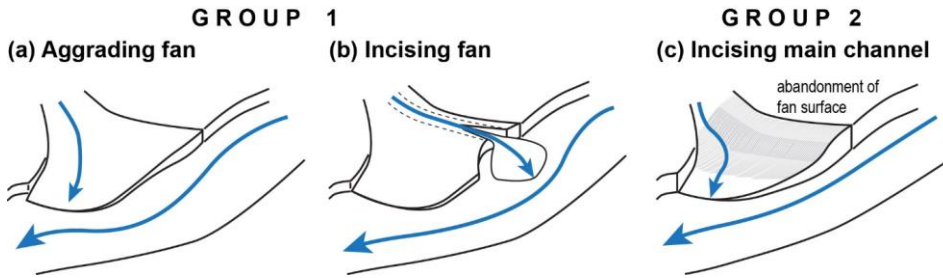
71 The dynamics of alluvial fans can introduce an additional level of complication to the
72 relationship between tributaries and main channels. Fans retain sediment from the tributary and
73 influence the response of the connected fluvial system to environmental perturbations (Ferguson
74 and Hoey, 2008; Mather et al., 2017). Despite the widespread use of alluvial fans to decipher
75 past environmental conditions (Bull, 1964; Colombo et al., 2000; D'Arcy et al., 2017; Densmore
76 et al., 2007; Gao et al., 2018; Harvey, 1996; Savi et al., 2014; Schildgen et al., 2016), we ~~still~~
77 lack a clear understanding of the interactions between alluvial fans and main channels under the
78 influence of different environmental forcing mechanisms. ~~The lack of a systematic analysis of~~
79 ~~these interactions represents a major gap in knowledge that hinders~~ ~~This knowledge gap limits~~
80 our understanding of (1) how channels respond to changes in water and sediment supply at
81 confluence zones, and (2) how sediment moves within fluvial systems (Mather et al., 2017;
82 ~~Simpson and Castellort, 2012~~), with potential consequences for sediment-transport dynamics as
83 well as ~~for~~ the composition and architecture of fluvial sedimentary deposits.

84 In this study, we analyze the interplay between a main channel and a tributary under different
85 environmental forcing conditions in an experimental setting, with particular attention to
86 tributaries that generate an alluvial fan. Physical experiments have the advantage of providing a
87 simplified setting with controlled boundary conditions ~~and~~ that may include water and sediment
88 discharge, and uplift rate or base-level changes. These models may thus capture many
89 components of complex natural behaviors (Hooke, 1967; Paola et al., 2009; Schumm and Parker,
90 1973), and they provide an opportunity to analyze processes at higher spatial and temporal
91 resolution than is generally possible in nature (e.g., De Haas et al., 2016; Parker, 2010; Reitz et
92 al., 2010). ~~These characteristics allow us) and~~ to directly observe connections between external
93 perturbations (e.g., tectonic or climatic variations) and surface processes impacting landscapes.

94 We present results from two groups of experiments in which we separately imposed a
95 perturbation either in the tributary only (Group 1, Fig. 1a, b) or solely in the main channel
96 (Group 2, Fig. 1c). Group 1 can be further subdivided into cases in which the tributary has: (a) an
97 aggrading alluvial fan (Fig. 1a*) or (b) an incising alluvial fan (Fig. 1b). ~~In this context, we~~
98 distinguish between two modes of fan construction: fan aggradation, i.e., deposition of material
99 on the fan surface, which leads to an increase in the fan surface elevation, and fan progradation,
100 i.e., deposition that occurs at the downstream margin of the fan, which leads to fan lengthening.
101 Progradation may occur during both aggradation and incision phases (Fig. 1). ~~1b), whereas~~ Group
102 2, in contrast, represents ~~athe~~ case of a sudden increase in water discharge in the main channel
103 (Fig. 1c). ~~These three cases represent what may occur in many natural environments (e.g.,~~
104 ~~Hamilton et al., 2013; Leeder and Mack, 2001; Mather et al., 2017; Schumm 1973; Van Dijk et~~
105 ~~al., 2009); 1c), as for example related to an increase in glacial melt.~~

106 By analyzing how a tributary may affect the main channel under these different forcing
107 conditions, we aim to build a conceptual framework that lends insight into the interplay between
108 alluvial fans and main channels. Toward this goal, we provide a schematic representation of how
109 the downstream delivery of sediment changes under different environmental conditions. Through
110 this representation, we hope to contribute to a better understanding and interpretation of fluvial
111 morphologies and sedimentary records, which may hold important information about regional
112 climatic and tectonic history (Allen, 2008; Armitage et al., 2011; Castelltort and Van Den
113 Driessche, 2003; Densmore et al., 2007; Mather et al., 2017; Rohais et al., 2012).

114



115

116 Figure 1. Schematic representation of the three scenarios analyzed in this study.

117

118 2. Background and Motivation

119 2.1. Geometry and sediment transfer dynamics in a single-channel system

120 2.1.1. General concepts

121 An alluvial river is considered to be in steady state (*equilibrium regime*) when its water
122 discharge provides sufficient power, or sediment-transport capacity, to transport the sediment
123 load supplied from the upstream contributing area at a given channel slope (Bull, 1979; Gilbert,
124 1877; Lane, 1955; Mackin, 1948). ~~When that power is insufficient, sediment is deposited within~~
125 ~~the channel (aggradation), whereas when the sediment transport capacity exceeds the sediment~~
126 ~~supply, the river erodes the channel banks and bed (incision) (Lane, 1955). Any change in~~
127 ~~sediment or water supply modifies the sediment to water ratio, such that~~ ~~When a perturbation~~
128 ~~occurs in the system,~~ the river must transiently adjust one or more of its geometric features (e.g.,
129 slope, width, depth, or grain-size distribution) to re-establish equilibrium (Mackin 1948; Meyer-
130 Peter and Müller, 1948).

131 ~~When a perturbation occurs in the system, slope~~ Slope adjustments are not uniform along the
132 channel. If the perturbation occurs ~~upstream in the basin's headwater~~ (e.g., a change in water or
133 sediment supply), ~~channel slope changes first at~~ adjustments propagate downstream from the
134 channel head ~~through incision or aggradation (e.g., (Simpson and Castelltort 2012; Tofelde et al.,~~

135 2019; Van den Berg Van Saparoea and Potsma, 2008; Wickert and Schildgen, 2019). ~~With~~
136 ~~time~~In contrast, slope adjustments ~~proceed-propagate upstream if a perturbation occurs toward~~
137 ~~the downstream until end of the entire channel slope has adjusted to the new condition.~~
138 ~~Conversely, when perturbations occur downstream (e.g., a change in base level), the slope~~
139 ~~initially changes at the channel mouth, and the slope adjustment propagates upstream until the~~
140 ~~entire channel is adjusted to the new base level) (Parker et al., 1998; Tofelde et al., 2019; Van~~
141 ~~den Berg Van Saparoea and Potsma, 2008; Whipple et al., 1998). The sediment transport rate of~~
142 ~~the river also depends on the direction of the change, as an increase or a decrease in precipitation~~
143 ~~or uplift rates trigger opposite responses (i.e., increase or decrease in sediment transport rate;~~
144 ~~Bonnet and Crave, 2003).~~

145 At the scale of a drainage network, these geometric adjustments may alter the mechanisms
146 and rates at which sediment is moved across landscapes. In general, under both steady and
147 transient conditions, sediment moves from zones of erosion to areas of deposition passing
148 through a *transfer zone* (Castelltort and Van Den Driessche, 2003). The capacity of the transfer
149 zone to temporarily store or release sediment can influence the amount and the provenance of
150 sediment reaching the depositional zone, buffering the sedimentary signal carried through the
151 system (Tofelde et al., 2019). This buffering may be particularly important for the outcome of
152 analyses that use the geochemical composition of sediment (e.g., cosmogenic nuclide
153 concentrations) to date fluvial deposits or infer changes in erosion rate (Biermann and Steig,
154 1996; Granger et al., 1996; Lupker et al., 2012; Wittmann and von Blanckenburg, 2009;
155 Wittmann et al., 2011).

156 Although our understanding of buffering within the sediment transfer zone helps to explain
157 how landscape perturbations are recorded in river morphology and downstream sedimentary
158 records, to date neither physical (Tofelde et al., 2019), theoretical (Castelltort and Van Den
159 Driessche, 2003; Paola et al., 1992; Wickert and Schildgen, 2019), nor numerical (Simpson and
160 Castelltort, 2012; Wickert and Schildgen, 2019) models take into account how the dynamics of
161 tributary junctions affect the geometry or sediment transport of the main channel. Tributary sub-
162 systems exist across spatial scales from small headwater catchments to continental-scale rivers
163 (i.e., short to large transfer zones). They may alter the amount of sediment entering the transfer
164 zone, modifying the sediment input signals that can be recorded by fluvial terraces and

165 sedimentary basins. Understanding how tributaries and their fans interact with the main channel
166 is critical to correctly reconstruct external forcing conditions from the sediments of alluvial fans,
167 fluvial terraces, and depositional sinks.

168 *2.1.2. Alluvial fans*

169 Alluvial fans typically form at points of rapid decrease of channel slope and/or increases in
170 valley width (Benda, 2008; Bull, 1964). Their depositional processes are characterized by a
171 combination of sheet flows and channelized flows that are interrupted by large reorganizations of
172 the channel system through avulsions (Bryant et al., 1995; De Haas et al., 2016; Hooke and
173 Rohrer, 1979; Reitz et al., 2010; Reitz and Jerolmack, 2012). Variations in these processes can
174 be related to the internal, i.e. autogenic, dynamics of the system (Hamilton et al., 2013; Kim and
175 Jerolmack, 2008; Van Dijk et al., 2009, 2012) or to external forcings (Armitage et al., 2011;
176 Rohais et al., 2012). In general, sheet flows deposit sediment uniformly over the entire fan
177 surface. Conversely, channelization on fans is generally associated with localized erosion.
178 Avulsions are sudden reorganizations of the channel system that are integral to the cyclic
179 construction of a fan (Straub et al., 2009). They occur when channels aggrade above the fan
180 surface and suddenly change position to start deposition on a new location of the fan surface
181 (Hamilton et al., 2013; Van Dijk et al., 2009).

182 ~~In our experiments, we distinguish between two modes of fan construction: fan aggradation,~~
183 ~~i.e., deposition of material on the fan surface, which leads to an increase in the fan surface~~
184 ~~elevation, and fan progradation, i.e., deposition that occurs at the downstream margin of the fan,~~
185 ~~which leads to fan lengthening. Progradation may occur during both aggradation and incision~~
186 ~~phases (Fig. 1).~~

187 2.2. Geometry and sediment-transfer dynamics in a multi-channel system

188 *2.2.1. Tributary influence on main channel*

189 At confluence zones, the main channel is expected to adapt its width, slope, sediment
190 transport rate, and sediment-size distribution according to the combined water and sediment
191 supply from the main channel and the tributary (Benda et al., 2004b; Best, 1986; Ferguson et al.,

192 2006; Lane 1955; Miller, 1958; Rice et al., 2008). Consequently, a perturbation occurring in the
193 tributary will also affect the main channel. ~~For example, a sudden increase in sediment input~~
194 ~~from a tributary (e.g., from a landslide or debris flow) can overwhelm the transport capacity of~~
195 ~~the main channel, thereby inducing sediment deposition at the confluence (Fig. 1a). As a result,~~
196 ~~the main channel upstream of the tributary experiences a rise in its local base level, which causes~~
197 ~~additional local deposition and a transient reduction in the main channel slope upstream of the~~
198 ~~tributary (Ferguson et al., 2006; Benda, 2008; Benda et al., 2004b). This sediment deposition~~
199 ~~upstream from the tributary increases the slope of the main channel downstream of the tributary,~~
200 ~~until the main channel is adjusted to transporting the higher sediment load (Benda et al., 2003;~~
201 ~~Ferguson et al., 2006; Ferguson and Hoey, 2008; Mackin, 1948; Rice and Church, 2001). It~~
202 ~~follows that the main channel both upstream and downstream from the tributary should undergo~~
203 ~~an aggradation phase, the former due to an increase in its local base level at the junction, the~~
204 ~~latter because of an increase in sediment supply from the tributary (Ferguson and Hoey, 2008;~~
205 ~~Mackin, 1948; Rice and Church, 2001). In their numerical model, Ferguson et al. (2006) In their~~
206 ~~numerical model, Ferguson et al. (2006) explored the effects that changes in sediment supplied~~
207 ~~from a tributary have on the main channel's slope. They~~ found that when tributaries cause
208 aggradation at the junction with the main channel, the main channel slope adjustments extend
209 approximately twice as far upstream as they do downstream. They additionally found that
210 variations in grain-size ~~input from aof the~~ tributary influence the grain-size distribution in the
211 main channel, both upstream and downstream of the tributary junction. ~~Considering that in our~~
212 ~~experiments~~ Because we used a homogeneous grain size in our experiments, the work of
213 Ferguson et al. (2006) complements our analyses.

214 Whether the tributary is aggrading, incising, or in equilibrium may also have important
215 consequences for *how* and *where* local fluvial deposits (i.e., alluvial-fan deposits or fluvial
216 terraces) reflect environmental signals. For example, when sediment is trapped within a
217 tributary's alluvial fan, the fan acts as a buffer for the main channel, and environmental signals
218 do not propagate from the tributary into the fluvial deposits of the main channel (Ferguson and
219 Hoey, 2008; Mather et al., 2017). In contrast, where the tributary and main channel are fully
220 *coupled* (i.e. all sediment mobilized in the tributary reaches the main channel), the signal
221 transmitted from the tributary can be recorded in the stratigraphy of the main river (Mather et al.,

222 2017). Hence, to correctly interpret fluvial deposits and to reduce ambiguity, an understanding of
223 the aggradational/incisional state of the tributary and how this state influences the main channel
224 is important. In this study, we aim to provide this information for different tributary states. The
225 presence of an alluvial fan may additionally cause a change in the main river location, pushing it
226 against the opposite side of the valley. This allows the fan to grow more in the downstream
227 direction of the main flow, contributing to a strong asymmetry in its morphology that may be
228 preserved in the stratigraphic record of the flood plain (Giles et al., 2016).

229 2.2.2. Main channel influence on tributary

230 The main channel influences a tributary primarily by setting its local base level. Therefore, a
231 change in the main-channel bed elevation through aggradation or incision represents a
232 downstream perturbation for the tributary, and tributary-channel adjustments will follow a
233 bottom-up propagation direction (Mather et al., 2017; Schumm and Parker, 1973). Typically, a
234 lowering of the main channel produces an initial phase of tributary-channel incision (Cohen and
235 Brierly, 2000; Fulkner et al., 2016; Germanoski and Ritter, 1988; Heine and Lant, 2009; Ritter et
236 al., 1995; Simon and Rinaldi, 2000), followed by channel widening (Cohen and Brierly, 2000;
237 Germanoski and Ritter, 1988), which occurs mainly through bank erosion and mass-wasting
238 processes (Simon and Rinaldi, 2000). As base-level lowering continues, the fan may become
239 entrenched, with the consequent abandonment of the fan surface and renewed deposition at a
240 lower elevation (Clark et al., 2010; Mather et al., 2017; Mouchené et al., 2017; Nicholas et al.,
241 2009) (Fig. 1c). In contrast, aggradation of the main channel may lead to tributary-channel
242 backfilling and avulsion (Bryant et al., 1995; De Haas et al., 2016; Hamilton et al. 2013; Kim
243 and Jerolmack, 2008; Van Dijk et al., 2009, 2012).

244 When a non-incising main channel (*non-incising main axial river* of Leeder and Mack, 2001)
245 is characterized by efficient lateral erosion, it can efficiently erode the fan downstream margin,
246 thereby “cutting” its toe (Larson et al., 2015) (*fan-toe cutting* hereafter) (Fig. 1b). This toe-
247 cutting shortens generally occurs in the up-valley side of the fan and increases the tributary
248 channel slope thus shortens it (Giles et al., 2016.) As a consequence, the increase in tributary
249 channel slope increases and so does its transport capacity in the tributary, which triggers an
250 upstream-migrating wave of incision. Fan-toe cutting may thus cause fan incision and a

251 consequent increase in sediment supply from the tributary to the main channel (*healing wedge*
252 hereafter; Leeder and Mack, 2001), in a process similar to that caused by an incising main
253 channel (*incising main axial river* of Leeder and Mack, 2001).

254 ~~2.2.3. Main channel and tributary interactions~~

255 ~~Changes that occur in the tributary as a consequence of incision of the main channel may~~
256 ~~alter the sediment supplied to the main river and create a series of autogenic feedback processes~~
257 ~~that are generally referred to as a *complex response* (Schumm, 1973; Schumm and Parker, 1973).~~
258 ~~These processes may form landforms such as cut and fill terraces that are not directly linked to~~
259 ~~the original perturbation (Schumm, 1973), thereby complicating the reconstruction of past~~
260 ~~environmental changes from such landforms. In our experiments, we analyze the changes~~
261 ~~occurring in a tributary during a phase of main channel incision to evaluate these potential~~
262 ~~feedbacks.~~

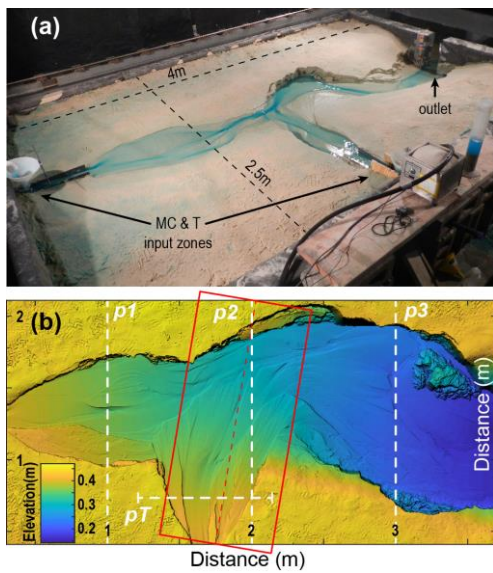
263 3. Methods

264 3.1. Experimental setup

265 We conducted physical experiments at the Saint Anthony Falls Laboratory (Minneapolis,
266 USA). The experimental setup consisted of a wooden box with dimensions of 4 m x 2.5 m x 0.4
267 m, which was filled with quartz sand with a mean grain size of 144 μm (standard deviation of 40
268 μm). Two separate water and sediment input zones were used to form a main channel (MC) and
269 a tributary channel (T) (Fig. 2a). The main channel's input zone was located along the short side
270 of the box, whereas the tributary's input zone was located along the long side at a distance of 1.7
271 m downstream of the main-channel inlet (Fig. 2a). This setting represents a landscape with two
272 transport-limited streams that join in a broad alluvial valley of unlithified/uncemented sediments;
273 common for many arid regions with large flood plains. A simplification in our experiments is
274 that the grain sizes from both the main stem and the tributary are equal. This will be further
275 discussed in section 5.4. For each of the two input zones, the water supply (Q_w) and sediment
276 supply (Q_{s_in}) could be regulated separately, and sand and water were mixed before entering the
277 box by feeding them through cylindrical wire-mesh diffusers filled with gravel. Before entering
278 the mesh, water was dyed blue to be visible on photos. At the downstream end, sand (Q_{s_out}) and

279 water exited the basin through a [fix](#) 20 cm-wide gap that opened onto the floor below. This
280 downstream sink was required to avoid deltaic sediment deposition that would, if allowed to
281 grow, eventually raise the base level of the fluvial system. At the beginning of each experiment,
282 an initial channel was shaped by hand to allow the water to flow towards the outlet of the box.

283



284

285 Figure 2. Experimental set-up. (a) Wooden box for the experiments showing the two zones of
286 sediment and water input, and the outlet of the basin. (b) Digital elevation model constructed
287 from laser scans (1 mm horizontal resolution). Red box shows the area of the swath grid used for
288 the calculation of the tributary long profile (Fig. 4) and slope values. Dashed white lines
289 represent the location of the cross sections shown in Figs. 5 and [S1 of the Supplementary](#)
290 [Material](#).

291

292 3.2. Boundary conditions

293 We performed six experiments with different settings and boundary conditions to simulate
294 different tributary–main-channel interactions- ([Table 1](#)). As a reference, we included one

295 experiment without a tributary and with a constant Q_{s_in} and Q_w (MC_NC, where MC stands for
296 *Main Channel only* and the suffix NC stands for *No Change* in boundary conditions; reported in
297 Tofelde et al., 2019 as the Ctrl_2 experiment). The other five experiments all have a tributary
298 and are divided into two groups: In Group 1, Q_w and Q_{s_in} on the main channel were held
299 constant, whereas we varied these inputs to the tributary. In Group 2, Q_w and Q_{s_in} on the
300 tributary were held constant, whereas we increased Q_w in the main channel. In natural systems,
301 changes in water and sediment supply may affect the main channel and tributary simultaneously,
302 but to isolate the effects of the main channel and the tributary on each other, we studied
303 perturbations that only affect one of them at a time. Our results can be combined to predict the
304 response to a system-wide change in boundary conditions.

305 Each group includes one experiment with no change (NC) in Q_{s_in} and Q_w (T_NC1 and
306 T_NC2, where T stands for *run with Tributary* and the numbers at the end correspond to the
307 group number). Group 1 includes one experiment with an increase followed by a decrease in
308 Q_{s_in} in the tributary (T_ISDS, where ISDS stands for *Increasing Sediment Decreasing Sediment*)
309 and one experiment with a decrease followed by an increase in Q_w in the tributary (T_DWIW,
310 where DWIW stands for *Decreasing Water Increasing Water*). Changes were first made in the
311 direction that favored sediment deposition and the construction of an alluvial fan. Group 2
312 includes one experiment with no change (T_NC2) and one with an increase in Q_w in the main
313 channel (T_IWMC, where IWMC stands for *Increasing Water in Main Channel*). Importantly,
314 the initial settings of the two groups of experiments are different (Table 1). The Q_{s_in} and Q_w
315 values were defined based on a set of preliminary test-runs and chosen to balance sediment
316 transport and sediment deposition. In particular, initial Q_w and Q_{s_in} of Group 2 guarantee a
317 higher Q_s/Q_w ratio compared to Group 1, so that we could evaluate the effects of a change in the
318 main-channel regime (from a *non-incising main river* to an *incising main river*) on the tributary
319 and on sediment-signal propagation. In the context of this coupled tributary–main-channel
320 system, we explore: 1) the geometric variations that occur in the main channel and in the
321 tributary (e.g., channel slope and valley geometry); and 2) the downstream delivery of sediment
322 and sedimentary signals.

323 **Table 1.** Overview of input parameters.

EXP NAME	Initial conditions				1 st change			2 nd change		Run time (spin-up)
	MC		T		MC	T		T		min
	Q _w	Q _{s_in}	Q _w	Q _{s_in}	Q _w	Q _w	Q _{s_in}	Q _w	Q _{s_in}	
	mL/s	mL/s	mL/s	mL/s	mL/s	mL/s	mL/s	mL/s	mL/s	
MC_NC**	95	1.3								690 (100)
<i>Non-incising mean axial rivers – Group1</i>					<i>(at 300 min)</i>			<i>(at 375* or 480 min)</i>		
T_NC1	95	1.3	63	2.2						600 (150)
T_ISDS	95	1.3	63	2.2			4.5		2.2	720 (150)
T_DWIW*	95	1.3	63	2.2		31.5		63		690 (150)
<i>Incising mean axial rivers - Group2</i>					<i>(at 180 min)</i>					
T_NC2	63	1.3	41.5	2.2						480 (100)
T_IWMC	63	1.3	41.5	2.2	126					480 (100)

Inserted Cells

Inserted Cells

Inserted Cells

324 * In the T_DWIW run the boundary condition change occurred at 375 min rather than 480 min
325 as in the T_ISDS experiment because fast aggradation that occurred at the tributary input zone
326 risked to overtop the wooden box margins.

327 **, Experiment published by Tofelde et al. (2019).

328

329 3.3. Measured and calculated parameters

330 3.2.1. Long profiles, valley cross-sections, and slope values

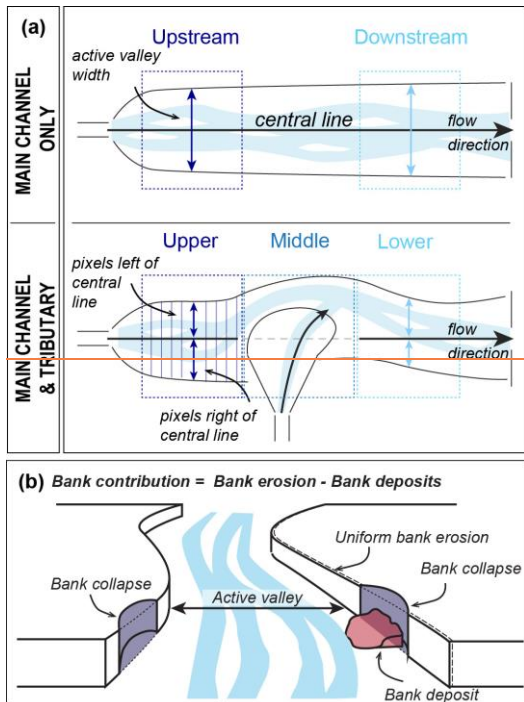
331 Every 30 min we stopped the experiments to perform a scan with a laser scanner mounted
332 on the railing of the basin that surrounded the wooden box. Digital elevation models (DEMs)
333 created from the scans have a resolution of 1 mm (Fig. 2b). We extracted long profiles and valley
334 cross sections from these DEMs (i.e., elevation profiles perpendicular to the main flow direction)
335 for the main channel and the tributary. Long profiles for the main channel were calculated by
336 extracting the lowest elevation point along each cross section along the flow direction. Long
337 profiles for the tributary were calculated with a similar procedure using outputs from
338 Topotoolbox's SWATH profile algorithm (Schwanghart and Scherler, 2014) at 1 mm spatial
339 resolution along the line of the average flow direction (Fig. 2b). By plotting elevation against
340 down-valley or down-fan distance, rather than along the evolving path of the channels, the
341 resulting slopes are slightly overestimated due to the low sinuosity of the channels. Cross
342 sections were extracted at fixed positions, perpendicular to the main flow direction, for both the
343 main channel and the tributary (Fig. 2b).

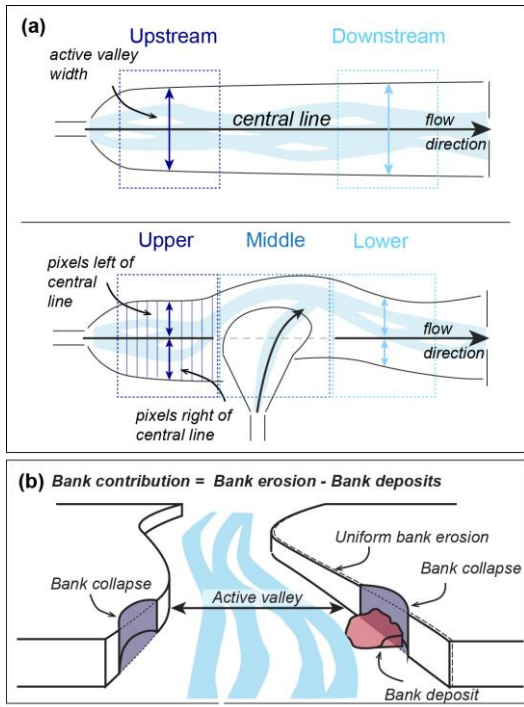
344 For the main channel, spatially-averaged slopes were additionally calculated by manually
345 measuring the bed elevation at the inlet and at the outlet of the wooden box at 10-minute
346 intervals during the experiments. This procedure yielded real-time estimates of channel slope.
347 For comparison, spatially-averaged slopes were subsequently calculated also for the tributary
348 channel using the maximum and minimum elevation of the tributary long profile calculated
349 within the SWATH grid. Slope data are reported in the supplementary material.

350 3.2.2. Active valley-floor width and symmetry

351 We defined the width of the active valley floor as the area along the main channel that was
352 occupied at least once by flowing water. It was measured along the main channel both upstream
353 and downstream of the tributary junction (Fig. 3a, upper panel). The active valley floor was
354 isolated by extracting all DEM values with an elevation of <0.42 m (where 0.42 m is the
355 elevation of the sand surface outside the manually-shaped channel) and with a slope of <15
356 degrees (a value visually selected from the DEMs as the best cut-off value for distinguishing the
357 valley floor from the banks). The average valley-floor width ~~values were~~ was then calculated as
358 the average sum of pixels in each of the 700 cross sections within the selected zones (i.e.,
359 upstream or downstream of the tributary junction; Fig. 3a, upper panel). The same method was
360 used to monitor valley axial symmetry. In this case, the averaged width was limited to the sum of
361 pixels to the left and to the right of an imaginary central line crossing the basin from the inlet to
362 the outlet (Fig. 3a). Small differences between left and right sums indicate high symmetry.

363





365

366 Figure 3. (a) Schematic representation of the method used to calculate the active valley width
 367 and axial symmetry. Symmetry and averaged width values are calculated for 700 cross sections
 368 located within the boxes marked in the upper panel. The averaged position of the valley margins
 369 with respect to an imaginary central line, which connects the source zone to the outlet of the
 370 wooden box, is shown in Figure 76. This representation highlights the symmetry of the valley
 371 and indirectly provides the valley width (i.e., sum of the right and left-margin positions). Boxes
 372 marked in the lower panel show the division into Upper, Middle, and Lower sections used for
 373 the calculation of the mobilized volumes (Fig. 98). (b) Schematic representation of the method
 374 used to calculate bank contribution: Elevation difference > -2.5 cm represents bank erosion and
 375 bank collapses, whereas differences > 2.5 cm represent large bank deposits. The contribution of
 376 the banks is calculated by subtracting these two values.

377

378 3.2.3. *Sediment discharge at the outlet (Q_{s_out}), mobilized volumes, and bank*
379 *contribution*

380 The sediment discharge at the outlet of the basin (Q_{s_out}) was manually recorded at 10-minute
381 intervals by measuring the volume of sediment that was collected in a container over a 10-second
382 period. Q_{s_out} was also calculated by differencing subsequent DEMs (generating a “DEM of
383 Difference”, or DoD) and calculating the net change in sediment volume within the DEM.
384 Although having a lower temporal resolution than the manual measurements (i.e., DoDs are
385 averaged over 30 minutes), this DEM-based calculation allowed us to identify zones of
386 aggradation and incision within the system and to calculate their volumes. For each DoD, we
387 distinguished between changes along the active valley floor due to channel dynamics (elevation
388 difference < 2.5 cm, value chosen as best cut-off value) and changes that occur along the channel
389 and valley walls, for example due to bank collapses (elevation difference > 2.5 cm). Changes
390 within the active valley floor were further divided into areas of net *aggradation* ($\Delta V_{vf} > 0$) and
391 net erosion ($\Delta V_{vf} < 0$). Changes in bank elevation were divided into net bank deposition ($\Delta V_b >$
392 0) and net bank collapses or erosion ($\Delta V_b < 0$). These were used to calculate the bank
393 contribution (V_b) to the total volume (V) of mobilized sediment (Fig. 3b). We separated the
394 upper, middle, and lower sections of the experimental river valley by dividing the DEMs into
395 three different zones (Fig. 3a, lower panel). For each section, we calculated the volume of net
396 change in sediment moved volumes between two time steps within the active valley floor (V_{vf}),
397 along the banks (V_b), and the sum of the two contributions ($V = V_{vf} + V_b$).

398 The volumes are normalized to the Q_{s_in} measured over 30 minutes (to match the 30-minute
399 period of a DoD). Negative V values indicate net incision, whereas positive values indicate net
400 aggradation. V values close to zero may indicate that there was no change, or that the net incision
401 \cong net aggradation. As such, it is important to look at the variations through time rather than at
402 single values.

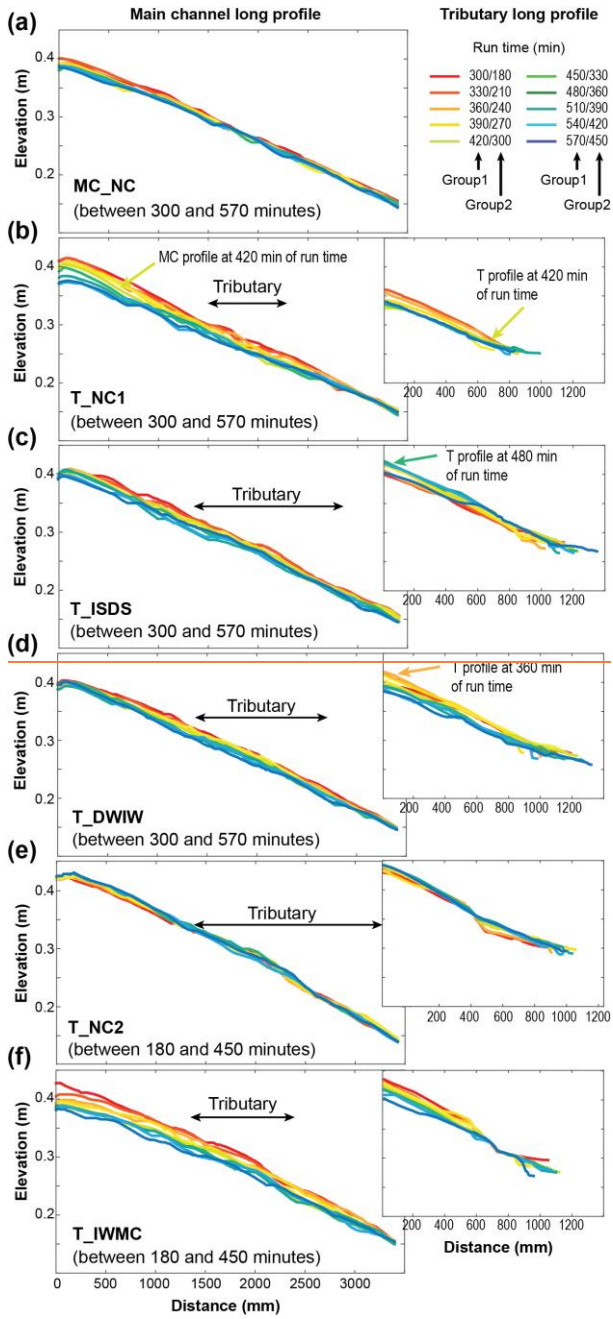
403 4. Results

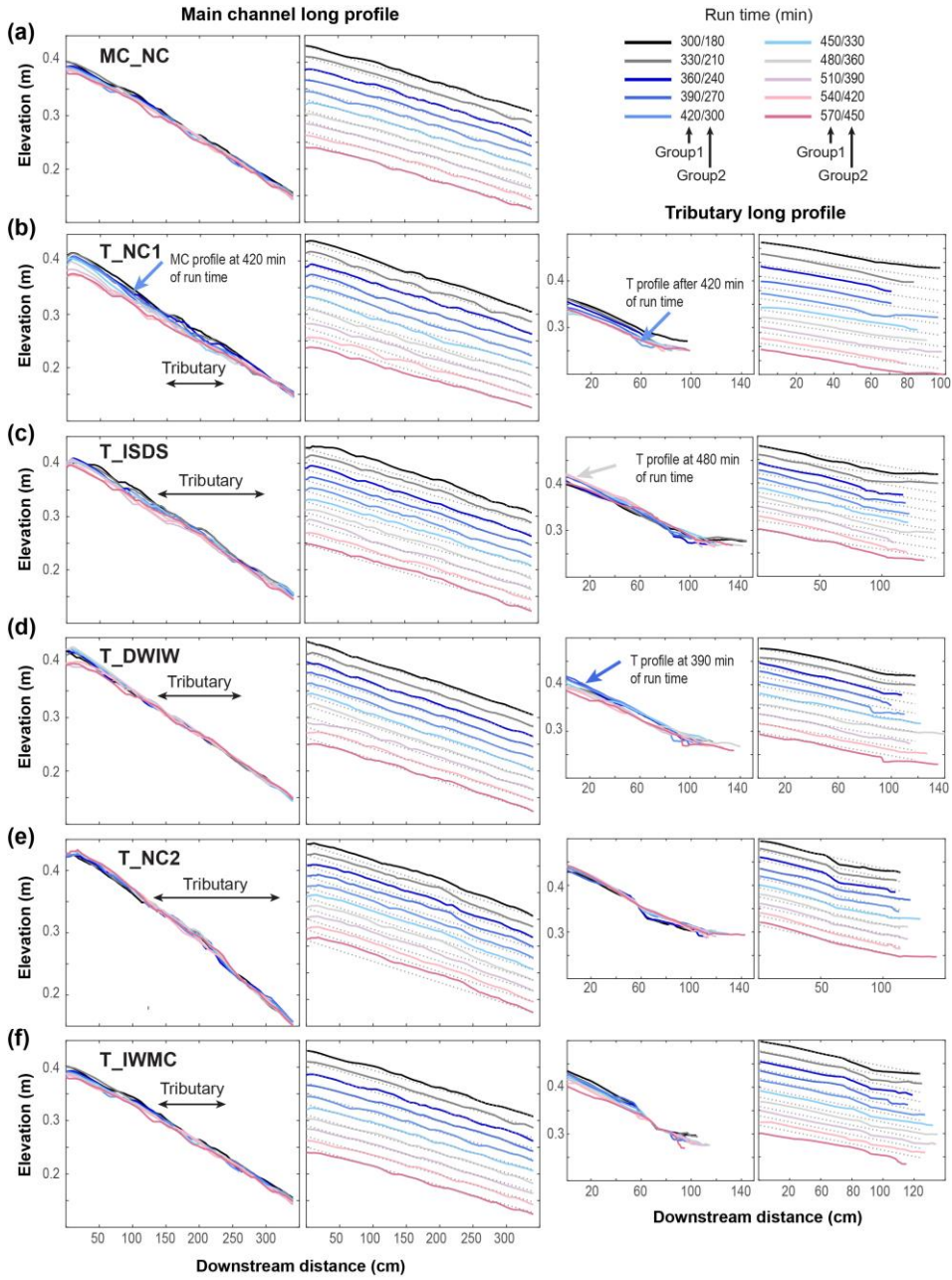
404 All experiments included an initial adjustment phase characterized by high Q_{s_out} and a
405 short and rapid increase in the main-channel slope through preferential channel incision at the
406 downstream end of the main channel. This phase represents the adjustment from the manually
407 constructed valley shape to the shape that is equilibrated to the imposed boundary conditions. At
408 the start of the adjustment phase, the channel rapidly incised toward the outlet, which was much
409 lower than the height of the manually constructed valley bottom, ~~meanwhile depositing.~~
410 ~~Meanwhile, the channel deposited~~ material at the channel head, adjusting to the Q_{s_in} and Q_w
411 values. Analogous to a base-level fall observed in nature, ~~this~~ ~~these changes~~ caused an increase in
412 main-channel slope near the outlet and the upstream migration of a diffuse knick-zone that
413 lowered the elevation of the main channel. After this initial adjustment, which marks the end of
414 the spin-up phase, the main controlling factors for the shape of the channel were the Q_{s_in} and Q_w
415 values only.

416 4.1. Geometric adjustments

417 ~~Channel~~ ~~Following the spin-up phase, channel~~-slope adjustments in our experiments
418 ~~followed~~ ~~matched~~ the theoretical models described above (Section 2.1). ~~Following the spin-up~~
419 ~~phase, the~~ ~~The~~ main-channel slope decreased in all experiments through incision at the upstream
420 end, except for T_NC2 and the initial phase of T_IWMC, in which the boundary conditions
421 favored aggradation (Fig. 4, Table 1). The slope of the tributary increased during periods of fan
422 aggradation (e.g., IS phase of the T_ISDS run, and DW phase of the T_DWIW run) and
423 decreased during periods of fan incision (DS phase of the T_ISDS run, and IW phase of the
424 T_DWIW run) (Fig. 4). Slope adjustments did not occur uniformly, but followed a top-down or
425 bottom-up direction depending on the origin of the perturbation (e.g., changes in headwater
426 conditions or base-level fall at the tributary outlet).

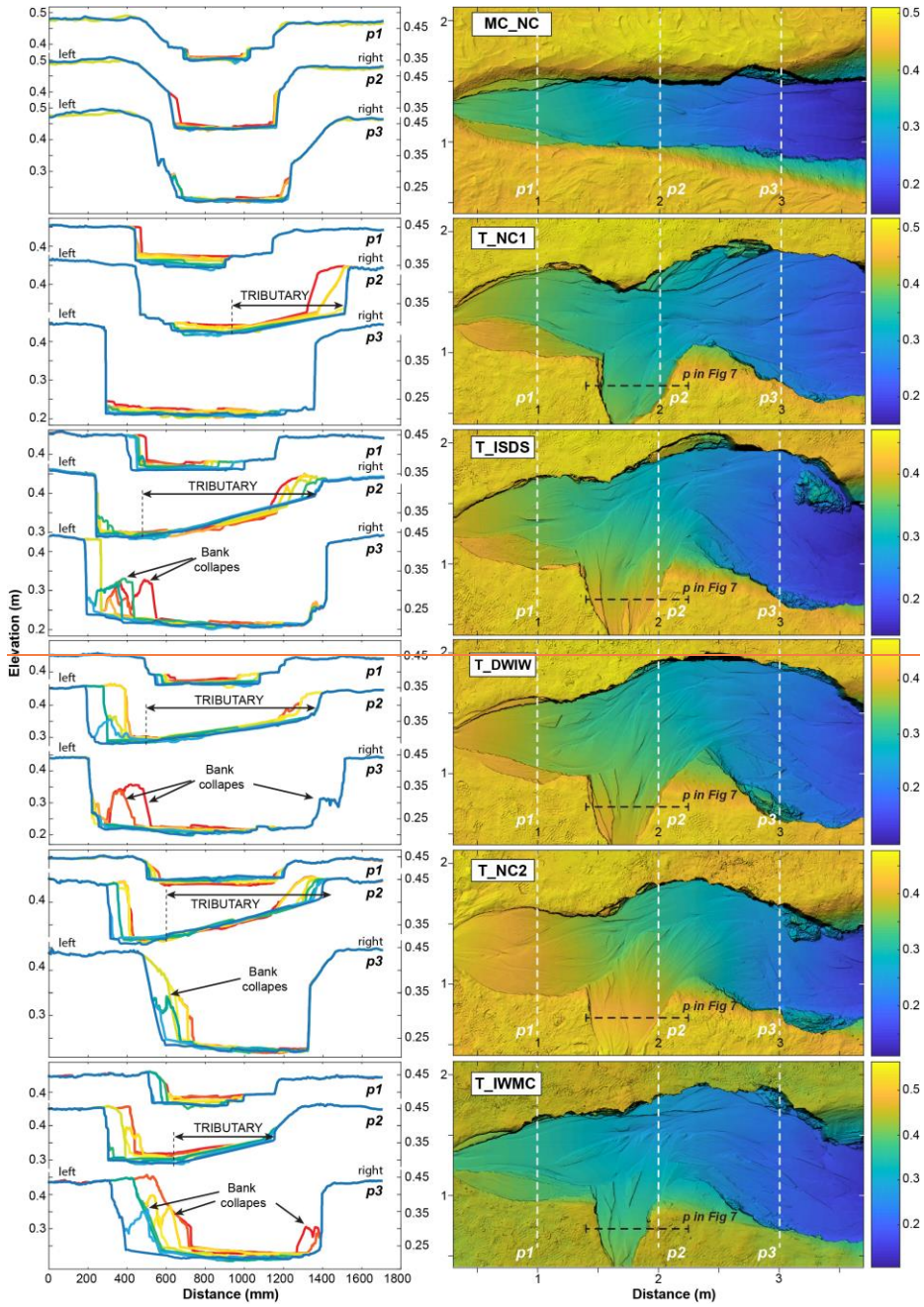
427

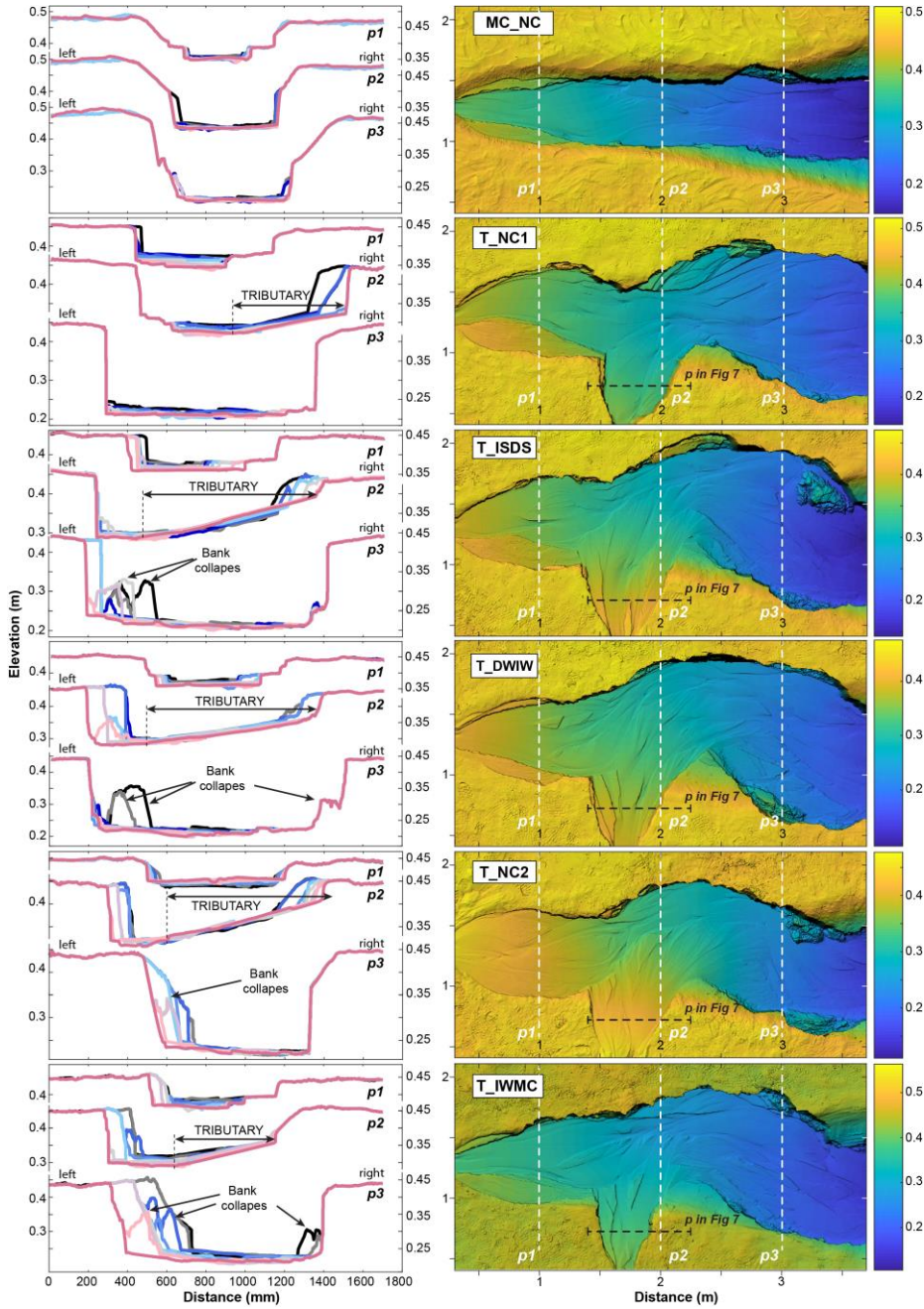




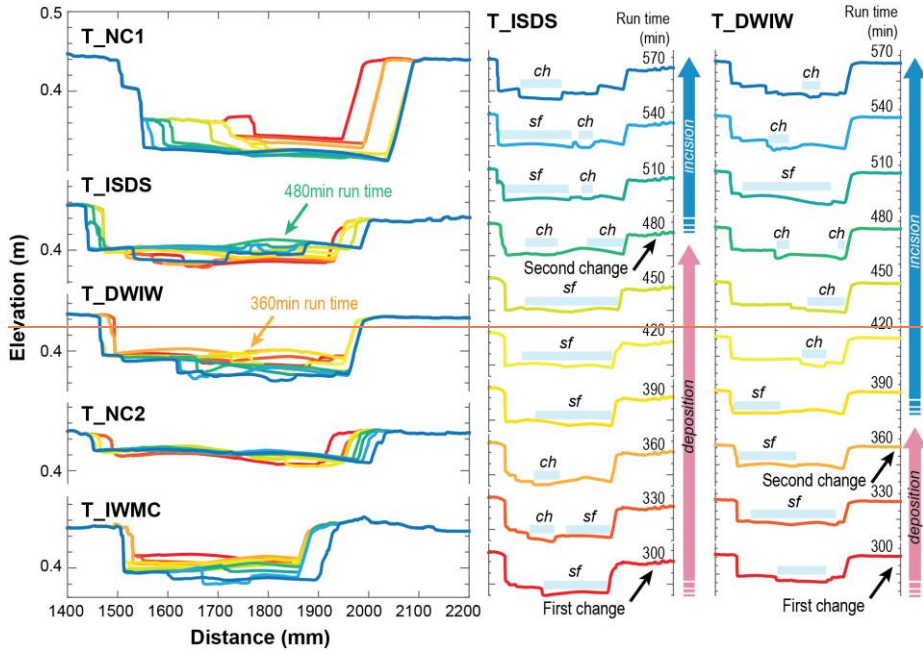
430 Figure 4. Long profiles of the main channel (left panels) and of the tributary channel (right
431 panels) for all runs. Profiles represent the experiments between 300 and 570 minutes for the
432 MC_Ctrl2, T_NC1, T_ISDS, and T_DWIW runs (legend values to the left of the slashes), and
433 between 180 and 450 minutes for the T_NC2, and T_IWMC runs (legend values to the right of
434 the slashes). For both the main and the tributary channel, left panels show the topographic
435 evolution of the channels with time, whereas right panels show a single profile (i.e., at a specific
436 time) compared to the average slope of the first plotted profile. Along the main channel profiles,
437 horizontal arrows indicate the position and extent of the tributary channel/alluvial fan, whereas
438 colored arrows indicate the position of the channels in particular run times discussed in the text.
439

440 Valley width in both the main channel (Fig. 5) and the tributary (Fig. 6S1 of the
441 Supplementary Material) increased during the experiments, ~~mainly~~ through bank erosion and
442 bank collapses, until reaching relatively steady values (Fig. 76). The experiments with the
443 tributary (Fig. 7b6b – f) developed a much wider main-channel valley, especially downstream of
444 the tributary, ~~where due to higher total Q_w was increased > 60% by the additional Q_w input~~
445 from compared to the tributary/main channel only experiments. In these experiments, valleys were
446 also strongly asymmetrical, with more erosion affecting the valley side opposite the tributary
447 (Figs. 5 and 76).
448



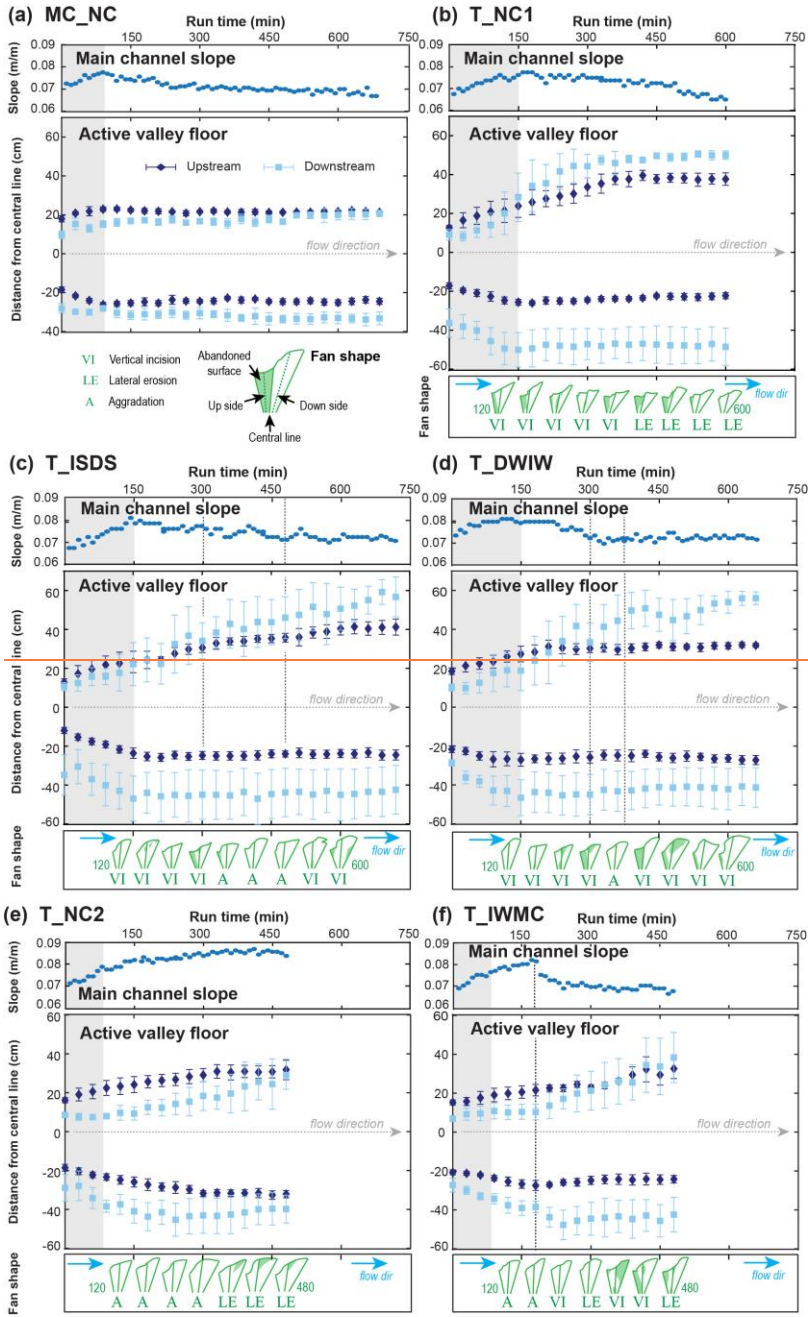


451 Figure 5. Left panels: Cross sections obtained from the DEMs at three different locations along
 452 the main channel (p1, p2, and p3 respectively). The color code represents successive DEMs as
 453 illustrated in Fig. 4 (i.e., same colors for the same run times). All cross sections are drawn from
 454 left to right looking in the downstream direction. Right panels: DEM maps expressed in meters;
 455 color code represents the elevation with respect to the channel floor (also in meters).

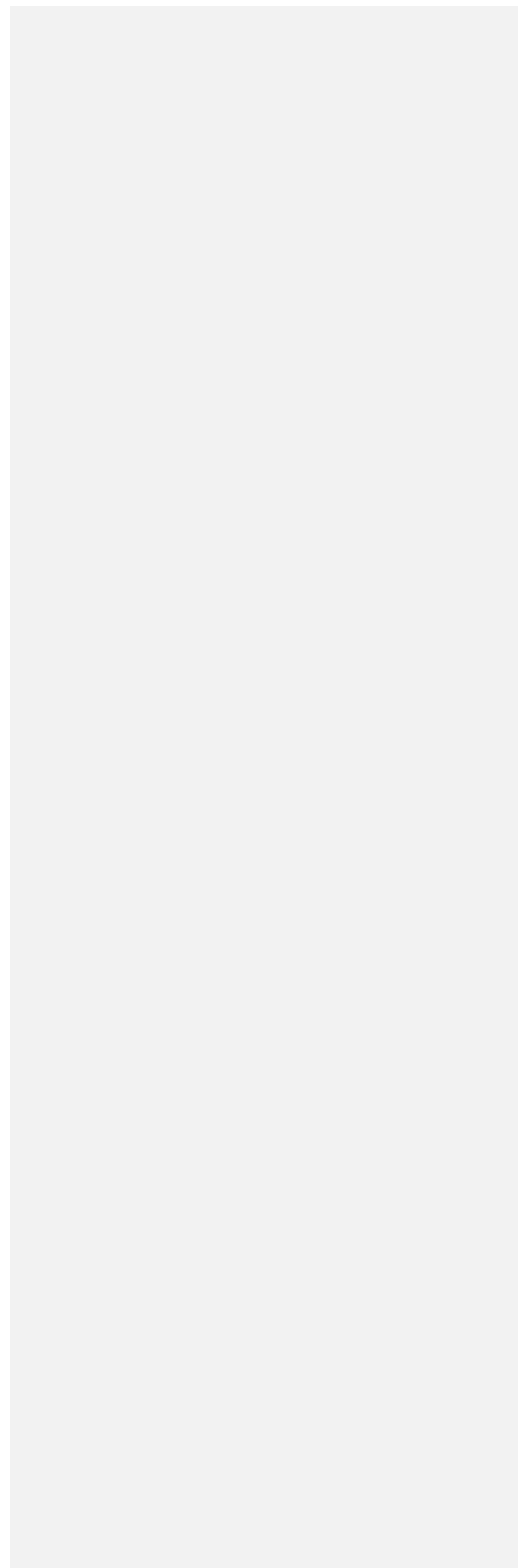


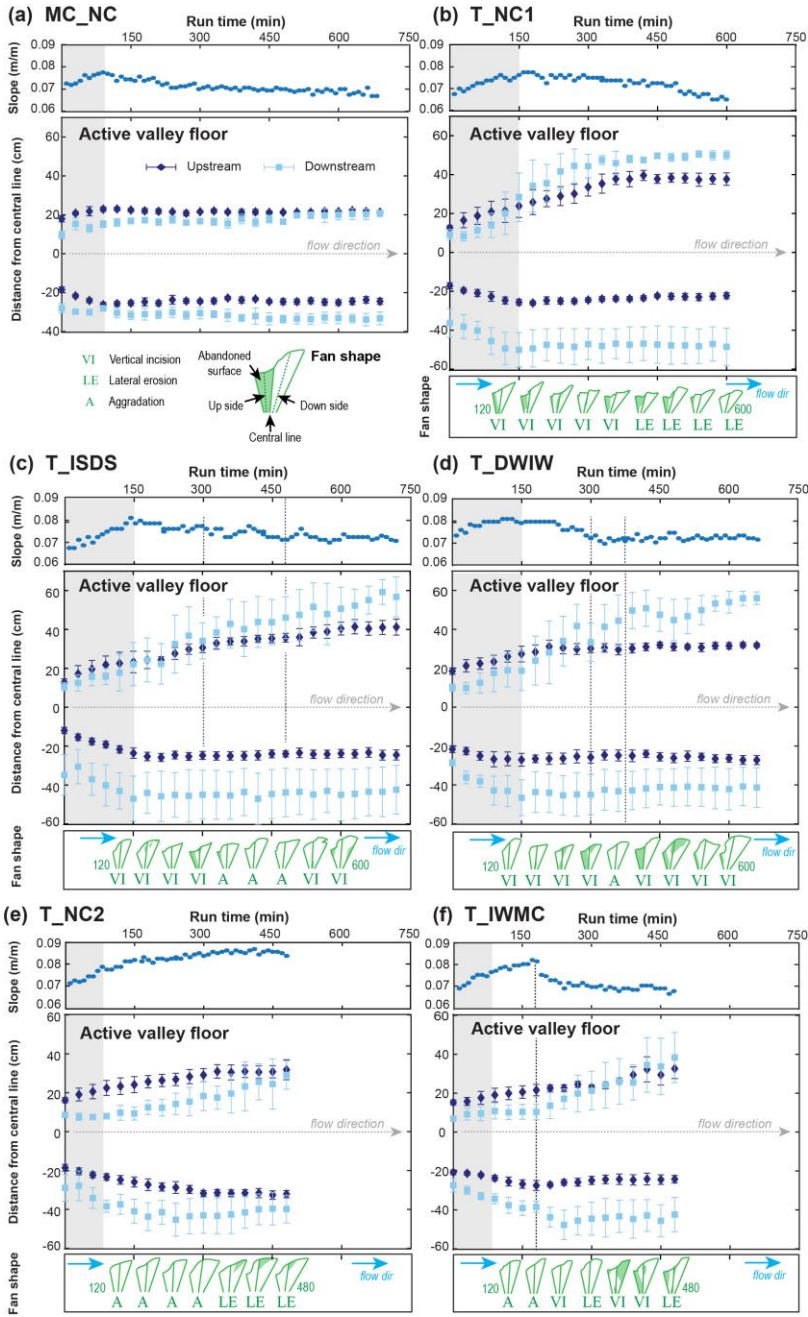
456
 457 Figure 6. Cross sections in the tributary drawn from left to right looking downstream. The left
 458 panels show the evolution of all runs (color code as in Fig. 4 and 5); the right panels show the
 459 evolution of the T_ISDS and T_DWIW runs in more detail: the ground surface elevation
 460 (colored lines) and the wetted areas (light blue bars) are shown. During aggradation, sheet flows
 461 (sf) dominate the transport mode of sediment, although channels (ch) may contemporaneously be
 462 present on the fan surface. During incision, the flow alternates between channelized flows and
 463 sheet flows and contribute to lowering the entire fan topography.

464



466 Figure 7.





468 [Figure 6](#). Variations in the geometry of the active valley floor for all experiments. For each
469 experiment the upper panel shows the measured slope (measured every 10 minutes during each
470 experimental run). The middle panel shows the calculated average position of the right and left
471 valley margins with respect to the central line, respectively for the main channel upstream and
472 downstream of the tributary junction (as indicated in Fig. 3a). Gray areas represent the spin-up
473 phase of each experiment (based on the break-in-slope registered through the manual slope
474 measurements; (a–f) upper panels). Vertical dotted lines in the T_ISDS, T_DWIW, and
475 T_IWMC runs represent the *time of change* in boundary conditions. Values are reported with
476 their relative 1σ value. For all experiments with a tributary, the shape of the fan and the dominant
477 sedimentary regime acting in the tributary at that specific time (i.e., vertical incision (VI), lateral
478 erosion (LE), or aggradation (A)) ~~is~~are shown in the lower panel. In all experiments, fan-toe
479 cutting (Leeder and Mack, 2001; Larson et al., 2015) mainly occurred at the upstream margin of
480 the fan and contributed to the strong asymmetry of the fan morphology (Table S9 of Supp.
481 Material), similar to what has been observed in nature (Giles et al., 2016).

482

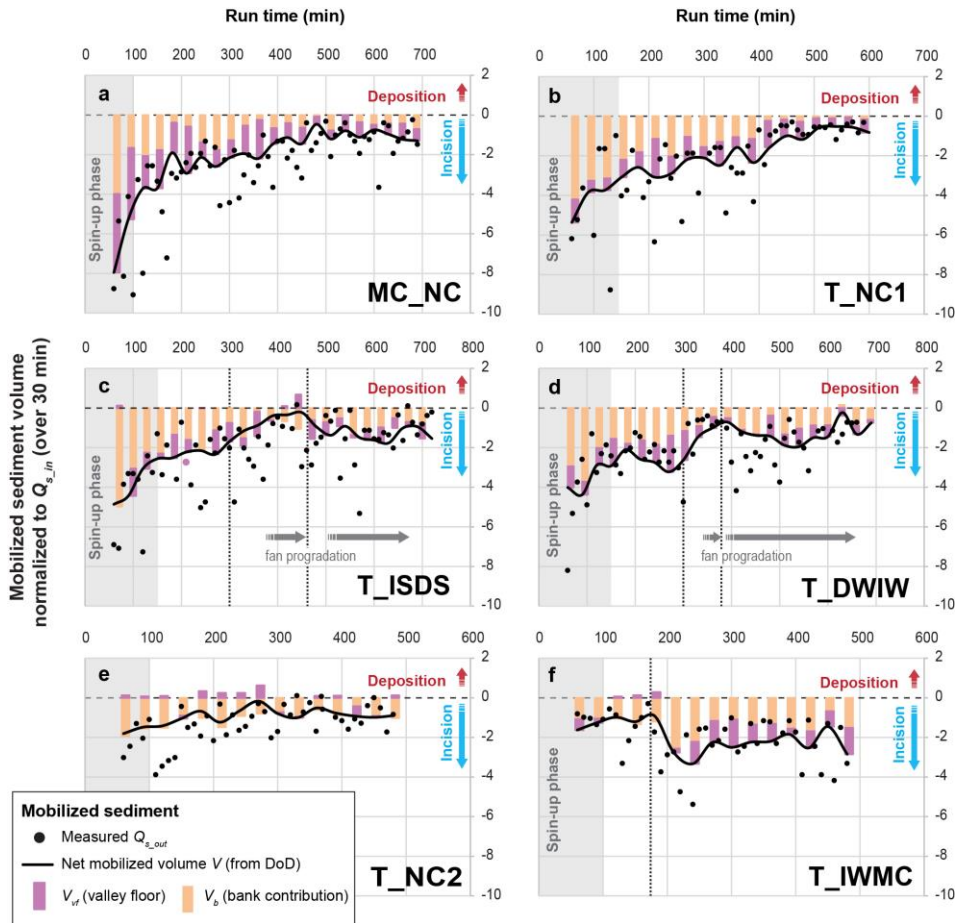
483 4.2. Q_{s_out} and bank contribution

484 Our experiments offered a rare opportunity to evaluate the impacts of sediment supply
485 from the tributary to the main channel through space and time. In general, sediment moved in
486 pulses, and areas of deposition and incision commonly coexisted (Fig. [8a7a](#)).

487 Q_{s_out} varied greatly, but generally decreased through time (the only exception is the
488 T_IWMC run, where Q_{s_out} remained high) (Fig. [87](#), black circles). Values for the mobilized
489 sediment, V , calculated from the DoDs (averaged over 30 minutes) show similar trends, but with
490 a lower variability that reflects the long-term average Q_{s_out} (Fig. [87](#), black lines). An appreciable
491 reduction of Q_{s_out} occurred when the system was approaching equilibrium (e.g., end of Fig.
492 [8a7a](#), b) and during times of fan aggradation in the tributary (i.e., IS and DW phases of Fig. [8e7c](#),
493 d, and e). Net mobilized sediment volumes (V) increased again during phases of fan incision (i.e.,
494 DS and IW phases of Fig. [8e7c](#) and d) and main-channel incision (e.g., IW phase in Fig. [8f7f](#)).
495 These increases were due to the combined effect of a general increase in sediment mobility
496 within the active valley floor (V_{vf}) and lateral erosion of the banks (V_b) (Fig. [87](#), violet and
497 orange bars respectively, and Fig. [S6S8](#) of the Supp. Material). The DoD analysis also indicates
498 that in all experiments, with the only exception of the MC run and of the phases approaching
499 steady-state, bank contribution was higher or of the same order of magnitude of the volume
500 mobilized in the valley floor (Fig. [87](#), orange and violet bars). This [observation](#) suggests that
501 bank erosion represented a major contribution to Q_{s_out} (Tables S3 to S8 of Supp. Material). ~~This~~

502 and is particularly true ~~also~~ for the T_NC2 run, where aggradation was favored, in which Q_{s_out} is
 503 dominated by the contribution of the banks (Fig. 8e7e, and Fig. 87S9 of the Supp. Material).

504



505

506 Figure 87. Volumes of sediment mobilized within the system. Black line: Net mobilized volume
 507 of sediment measured using the DoD. For comparison, black dots represent the Q_{s_out} values
 508 measured every 10 minutes (part of the difference between measured and calculated Q_{s_out} values
 509 may be due to the contribution of the most downstream area of the wooden box, which was
 510 shielded in the DEM reconstruction). Horizontal arrows indicate the timespan of fan
 511 progradation either during fan aggradation or fan incision. Vertical pointed lines represent the
 512 time of change in boundary conditions; horizontal dashed line separates aggradation and erosion.

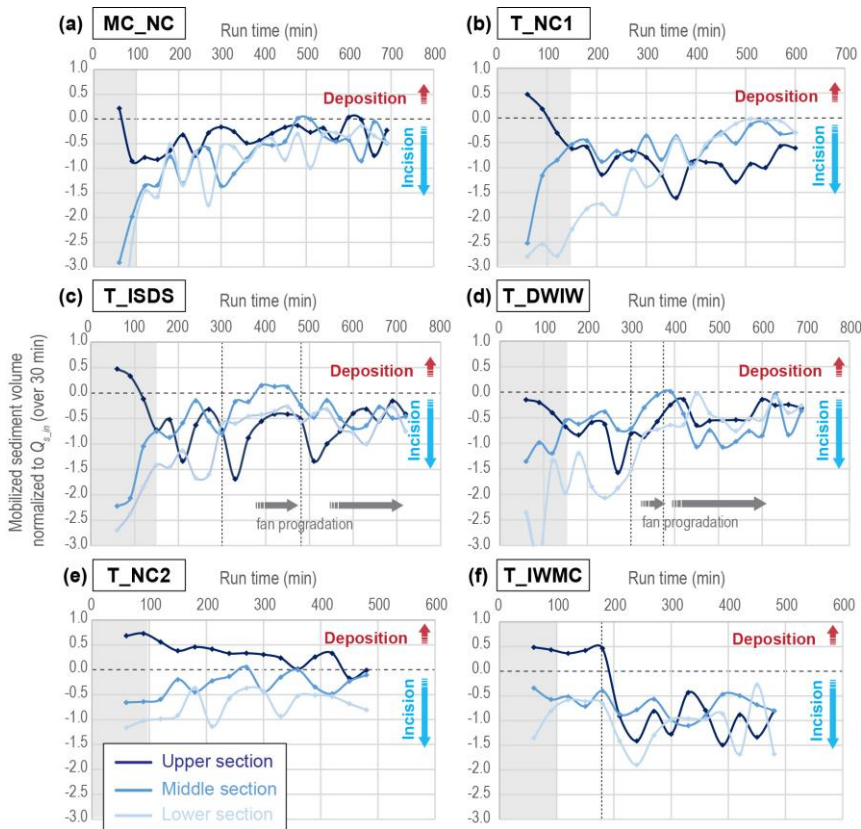
513

514 4.3. Downstream sediment propagation

515 To analyze the effects of the tributary on the mobility of sediment within the coupled
516 tributary–main-channel system, we monitored the volumes of sediment mobilized (V) in the
517 upper, middle, and lower sections of the fluvial network through time (Fig. 98). The complex
518 pattern of V in the different sections yields insights into downstream sediment propagation,
519 especially when coupled with maps of the spatial distribution of eroded and deposited sediment
520 (Fig. 10, and Figs. S1S2 to S5S7 in the Supp. Material):

- 521 1. In all experiments, including the one without a tributary (MC_NC), sediment moved in
522 pulses through the system (Fig. 98). As such, the mobilized volumes (V) of each section
523 can be *in-phase* or *out-of-phase* with the volumes mobilized in the others sections
524 (Castelltort and Van Den Driessche, 2003) depending on where the “pulse” of sediment
525 was located within the floodplain (Fig. 11a9a).
- 526 2. The sediment mobilized in the middle and lower sections of the T_NC1 run showed a
527 decrease in V after ca. 400 min, whereas in the upper section V remained nearly constant
528 (Fig. 9b8b), despite a marked increase in V_{vf} (Fig. S6S8 of Supp. Material).
- 529 3. In the T_ISDS run, the middle section showed, as expected, a strong reduction in V after
530 the onset of increased $Q_{s, in}$ in the tributary and consequent fan aggradation (300 to 480
531 minutes). Conversely, it showed an increase in V following the decrease in $Q_{s, in}$ and
532 consequent fan incision (480 minutes to the end of the run) (Fig. 9e8c). A similar pattern
533 can be seen in the lower section, with a reduction in V during fan aggradation and an
534 increase in V during fan incision. Interestingly, the upper section showed two peaks of
535 enhanced V (i.e., increase in sediment export) just after the changes in the tributary,
536 followed by a prolonged reduction of V (i.e., decrease in sediment export) during phases
537 of fan progradation.
- 538 4. Patterns similar to those described for the T_ISDS can be seen for the T_DWIW run.
539 However, due to the type of change in the tributary (i.e., decrease in Q_w , which increases
540 the Q_v/Q_w ratio, reducing the sediment-transport capacity) and due to the shorter duration
541 of the perturbation (300 to 375 minutes), the first peak of enhanced V in the upper
542 section was barely visible, whereas the second peak was not present. Rather, the upper

- 543 section shows a continuous decrease in V until ca. 420 min, i.e., circa 45 minutes after
 544 the onset of increased Q_w in the tributary (Fig. 9d8d and Fig. S3S5 of Supp. Material).
 545 5. The T_NC2 experiment is dominated by aggradation and V values are rather constant;
 546 (Fig. 9e8e and Fig. S4S6 of Supp. Material). Similar to the final part of the T_NC1 run,
 547 the upper section of the main channel showed a general increasing trend in V_{vf} (Fig. S7S9
 548 of Supp. Material).
 549 6. In the T_IWMC experiment, as expected, V increased immediately after the increase in
 550 Q_w in main channel in all three sections (indicating major incision), but was particularly
 551 evident in the upper and lower sections of the main channel (Fig. 9f8f).
 552

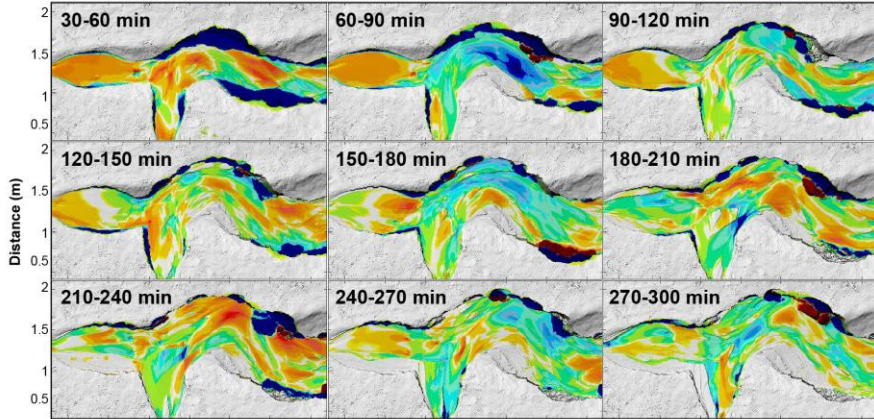


553

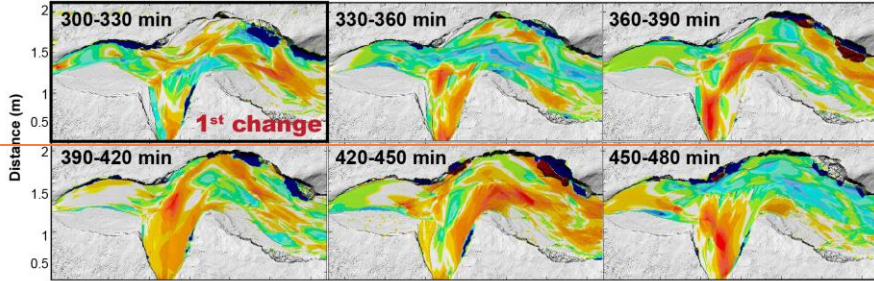
554 Figure 98. Volume (V) of sediment mobilized in each section (e.g., upper, middle, and lower
555 sections). Vertical lines represent the *times of change* in boundary conditions; horizontal dashed
556 line separates aggradation and erosion.

557

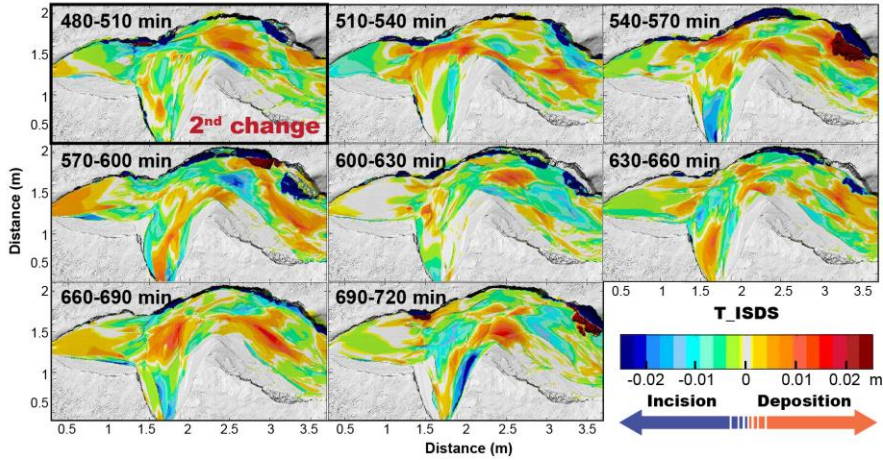
(a) $Q_{s_in\ (TRIBUTARY)} = 2.2\ \text{mL/s}$



(b) **Increasing sediment** ($Q_{s_in\ (TRIBUTARY)} = 4.5\ \text{mL/s}$)



(c) **Decreasing sediment** ($Q_{s_in\ (TRIBUTARY)} = 2.2\ \text{mL/s}$)



559 Figure 10. Sediment transfer dynamics within the system in the T-ISDS experiment (from DoDs
560 analysis). Variations between -0.001 and $+0.001$ m are considered as “no change” (in gray) to
561 account for the DEMs accuracy (i.e., 1 mm resolution). (a) Pre-perturbation phase (between 30
562 and 150 minutes is considered to be the spin-up phase); (b) Fan aggradation (300–390 min) and
563 progradation (390–480 min) phase; (c) Fan incision and progradation phase (480 min until end of
564 run).

566 5. Discussion

567 Our six experiments provide a conceptual framework for better understanding how tributaries
568 interact with main channels under different environmental forcing conditions (Fig. 1). We
569 particularly considered geometric variations of the two subsystems (i.e., tributaries and main
570 channels) and the effects of tributaries on the downstream delivery of sediment within the fluvial
571 system.

572 5.1. Aggrading and incising fans: geometrical adjustments and tributary–main- 573 channel interactions

574 In our experiments, the aggrading alluvial fans strongly impacted the width of the main-
575 channel valley both upstream and downstream of the tributary junction. By forcing the main
576 channel to flow against the valley-wall opposite the tributary, bank erosion was enhanced;
577 (Tables S3 to S8 and Fig. S8 in the Supp. Material), thus widening the main-channel valley floor
578 (Figs. 4, 76, and 49S4). Bank erosion and valley widening in the main channel also occurred
579 during periods of fan incision (Figs. 40b, S3S4b, S5, and S6S8 of the Supp. Material). We
580 hypothesize that this widening was related to pulses of sediment eroded from the fan, which
581 periodically increased the sediment load to the main channel and helped to push the river to the
582 side opposite the tributary (Grimaud et al., 2017; Leeder and Mack, 2001). Once there, the river
583 undercut the banks, causing instability and collapse. As such, periods of fan incision triggered a
584 positive feedback between increased load in the main channel and valley widening, which
585 occurred mainly through bank erosion and bank collapses. In these scenarios, bank contribution
586 (V_b) in the middle and lower sections of the main channel can be equal to, or larger than, the
587 sediment mobilized within the active valley floor (V_{vf}) (also for the T_NC2 run; Fig. 867b and
588 Fig. S6S8 and S7S9, Supp. Material). It follows that the composition of the fluvial sediment may

589 be largely dominated by material mobilized from the valley walls, with important consequences,
590 for example, for geochemical or provenance studies (Belmont et al., 2011).

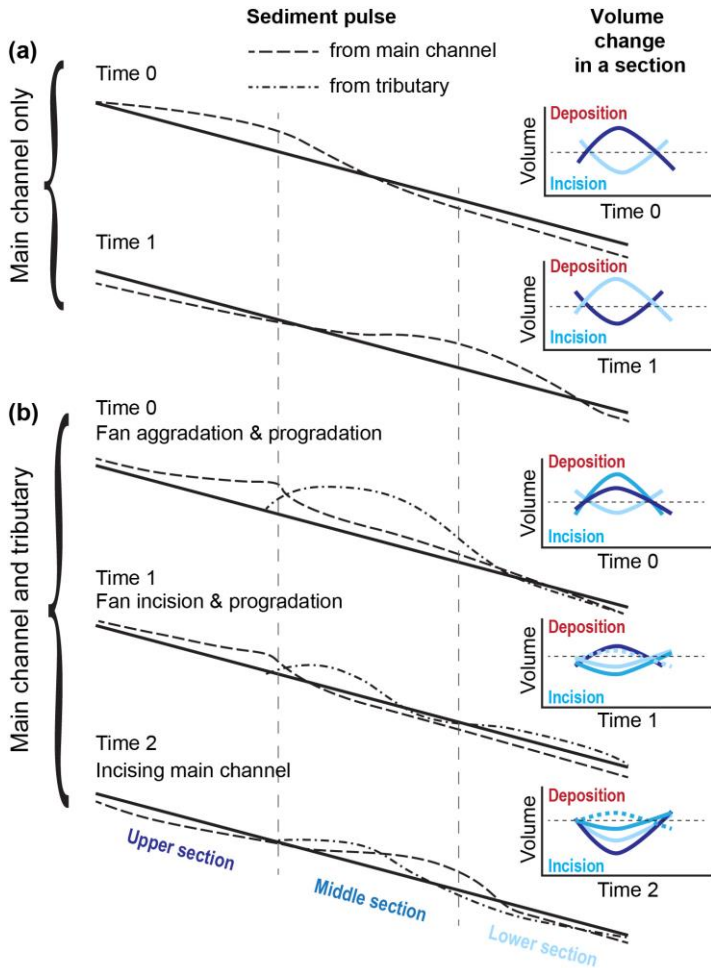
591 Our analysis of sediment mobility within the different sections of the main channel
592 highlighted that the presence of the alluvial fan affects the time needed to reach equilibrium in
593 the different reaches of the main river: in the T_NC1 run, for example, due to the sediment input
594 from the tributary, the middle and lower sections have a higher Q_s/Q_w ratio (0.022) than the
595 upper section (0.014), and may reach equilibrium faster (Gilbert, 1877; Wickert and Schildgen,
596 2019). Once the tributary [channel-profile](#) reached equilibrium (e.g., at ca. 420 minutes for
597 T_NC1; inset of Fig. 4b), the upper main channel rapidly adjusted by decreasing the elevation of
598 its channel bed (Fig. 4b) and increasing the sediment mobilized (Fig. [9b8b](#) and Fig. [S6S8](#) of
599 Supp. Material). This result suggests that equilibrium time scales of channels upstream and
600 downstream of tributaries can vary (Schumm, 1973), and that in a top-down direction of
601 adjustments, the equilibrium state of the upper section may be dictated by the equilibrium state
602 of its lower reaches because of the tributary influence.

603 In our experiments, fans were built under conditions that caused deposition at the tributary
604 junction (e.g., an increase in Q_{s_in} or decrease in Q_w in the tributary). When the perturbation
605 lasted long enough (e.g. in experiment T_ISDS), the fan prograded into the main channel. The
606 passage from fan aggradation to progradation was delayed relative to the onset of the
607 perturbation by the time necessary to move the sediment from the fan head to the fan margin
608 (e.g. for > 60 min in T_ISDS; Fig. [40bS4b](#)). This delay allowed for a temporarily efficient
609 transfer of sediment within the main channel (as marked by the peak in V of the upper main
610 channel section; Fig. [9e8c](#)). For tributaries subject to a change that caused tributary incision (e.g.,
611 decrease in Q_{s_in} or increase in Q_w), the elevation of the fan surface was progressively lowered
612 (inset of Fig. 4c and d, and Fig. [6S1 in the Supp. Material](#)), and the fan prograded into the main
613 channel with cyclic pulses of sediment discharge (e.g., Fig. [40eS4c](#)) (Kim and Jerolmack, 2008).
614 Progradation was generally localized where the tributary channel debouched into the main river
615 (e.g., depositing the *healing wedge* of Leeder and Mack, 2001), generally shortly after (< 30 min)
616 the onset of the perturbation (Figs. [40eS4c](#) and [S3S5](#) of the Supp. Material). When the fan
617 prograded, sediment in the main channel was [partially](#) blocked above the tributary junction (e.g.,
618 at 390 to 480 min in Fig. [40b. S4b](#), and at 510 min to the end of the run in Fig. [40e S4c](#); Fig. [S4S6](#)

619 of Supp. Material), and the upstream main-channel section experienced a prolonged decrease in
620 sediment mobility due to localized aggradation (Fig. 9e8c and d, and Fig. 44b9b).

621 Given the relative size of the tributary and main channel in our experiments (Q_w tributary ~
622 $2/3 Q_w$ main channel) and the magnitude of the perturbations (doubling of Q_{s_in} or halving of
623 Q_w), the impact of perturbations in the tributary on the sediment mobility (V) within the main
624 channel remained mostly within autogenic variability (Fig. 8b7b, Group 1). This observation
625 highlights how the analysis of changes in Q_{s_out} alone (for example inferred from the stratigraphy
626 of a fluvial deposit) may not directly reflect changes that occurred in the tributary, but can be
627 overprinted by autogenic variability. However, the analysis of V within individual sections of the
628 main channel, and particularly within the confluence zone (i.e., middle section), together with the
629 analysis of how sediment moves in space, reveal important changes in the sediment dynamics of
630 the main channel that may help to reconstruct the perturbations that affected the tributary
631 (Section 5.2; Figs. 98 and 44b9b). This observation underscores the need to study a range of
632 sedimentary deposits of both the tributary and main-channel ~~deposits~~ (Mather et al., 2017), both
633 upstream and downstream of a tributary junction.

634



635

636 Figure 449. Schematic representation of the average sediment mobilized in each section of the
 637 main channel. Solid black line represents the idealized equilibrium profile of the main channel,
 638 whereas dashed lines represent the volumes mobilized from the main channel and from the
 639 tributary. (a) Sediment dynamics in a single-channel system: sediment moves in pulses and upper
 640 and lower sections may be *out-of-phase* or *in-phase* depending on the dynamics of the middle
 641 section (i.e., the *transfer zone* of Castellort and Van Den Driessche, 2003). (b) Sediment
 642 dynamics in a tributary-main channel system: *Time 0* represents the “aggrading (and prograding)
 643 fan” scenario, where the upper and middle sections of the main channel undergo aggradation,
 644 while the lower section undergoes incision. *Time 1* represents the “incising (and prograding) fan”
 645 scenario, where the upper section may still be aggrading by it also starts to get incise creating a
 pulse of sediment that reaches the lower section. The middle section clearly sees an increase in

647 incision due to the imposed perturbation, while the lower section may undergo incision or
648 aggradation depending on the amount of sediment delivered from the fan, from the upper section,
649 and from bank erosion. *Time 2* represents the “incising main channel” scenario, where the fan
650 loses its influence on the dynamics of the main channel and both upper and lower sections
651 undergo incision. The middle section can undergo aggradation or incision depending on the
652 amount of sediment mobilized in the tributary and on the pulse of sediment moving from the
653 upper to the lower section of the main channel.

654

655 5.2. Incising main channel: geometric adjustments and tributary–main-channel 656 interactions

657 The main-channel bed elevation dictates the local base level of the tributary, such that
658 variations in the main-channel long profile may cause aggradation or incision in the tributary
659 (Cohen and Brierly, 2000; Leeder and Mack, 2001; Mather et al., 2017). In our experiments,
660 lowering of the main-channel bed triggered tributary incision that started at the fan toe and
661 propagated upstream (insets in Fig. 4). Because tributary incision increases the volume of
662 sediment supplied to the main channel, a phase of fan progradation would be expected, similar to
663 the cases described above (and in the *complex response* of Schumm, 1973). However, in our
664 experiment (i.e., T_IWMC), progradation did not occur: instead, the fan was shortened (Fig.
665 [SS7](#) Supp. Material). We hypothesize that the increased transport capacity of the main river
666 resulted in an efficient removal of the additional sediment from the tributary, thereby mitigating
667 the impact of the increased sediment load supplied by the tributary to the main channel. Another
668 consequence is that the healing wedge of sediment from the tributary is likely not preserved in
669 the deposits of either the fan margin or the confluence zone, hindering the possibility to
670 reconstruct the changes affecting the tributary. However, some insight can be obtained from the
671 analysis of sediment mobility. During main-channel incision, whereas both upper and lower
672 sections of the main channel registered a marked increase in V following the perturbation, the
673 middle section showed only minor variations (Fig. [9f](#)). We hypothesize that this lower
674 variability was due to the buffering effect of the increased load supplied from the fan undergoing
675 incision (i.e., caused by the sudden base-level fall that followed main-channel incision) (Fig.
676 [H9b](#)). In contrast, when incision in the tributary was caused by a perturbation in its headwaters,
677 V initially increased and then showed a prolonged decrease in the upper section during fan
678 aggradation, whereas it increased in the middle section during fan incision. These differences

679 may help to discern the cause of fan incision (i.e., either a perturbation in the main channel or in
680 the tributary).

681 We did not observe the *complex response* described by Schumm (1973), characterized by
682 tributary aggradation following incision along the main channel. ~~That~~The complex response in
683 Schumm's experiments likely occurred because the main river had insufficient power to remove
684 the sediment supplied by the tributaries, as opposed to what occurred in our experiments. When
685 aggradation occurs at the tributary junction, one may expect to temporarily see an evolution
686 similar to that proposed in the "aggrading alluvial fan" scenario, with the development on an
687 alluvial fan that may alter the sediment dynamics of the main channel, modulating the sediment
688 mobilized in the upper and lower sections of the river and delaying main-channel adjustments. In
689 our experiment, instead, a prolonged erosional regime within the main channel may have led to
690 fan entrenchment and fan-surface abandonment (Clarke et al., 2008; Nicholas and Quine, 2007;
691 Pepin et al., 2010; Van Dijk et al., 2012). Despite the lack of fan progradation, an increase in
692 bank contribution following incision of the main channel did occur (Fig. ~~S7b~~6, Fig. ~~S7S9~~ Supp.
693 Material) and could be explained by (1) higher and more unstable banks and (2) an increased
694 capacity of the main channel to laterally rework sediment volumes under higher water discharges
695 (Bufe et al., 2019).

696 5.3. Sediment propagation and coupling conditions

697 Understanding the interactions between tributaries and main channel, and the contribution of
698 these two sub-system to the sediment moved (either eroded or deposited) in the fluvial system, is
699 extremely important for a correct interpretation of fluvial deposits (e.g., cut-and-fill terraces or
700 alluvial fans), which are often used to reconstruct the climatic or tectonic history of a certain
701 region (e.g., Armitage et al., 2011; Densmore et al., 2007; Rohais et al., 2012); Simpson and
702 Castelltort, 2012).

703 In their conceptual model, Mather et al. (2017) indicate that an alluvial fan may act as a
704 *buffer* for sediment derived from hillslopes during times of fan aggradation, and as a *coupler*
705 during times of fan incision, thereby allowing the tributary's sedimentary signals to be
706 transmitted to the main channel. From our experiments, we can explore the effects that tributaries
707 have not only in storing or releasing sediment to the main channel, but also in modulating the
708 flux of sediment within the fluvial system. In doing so, we create a new conceptual framework

709 that takes into account the connectivity within a coupled alluvial fan-main channel system and
710 the mechanisms with which sediment and sedimentary signals may be recorded in local deposits
711 (Fig. 4210). Results are summarized as follows:

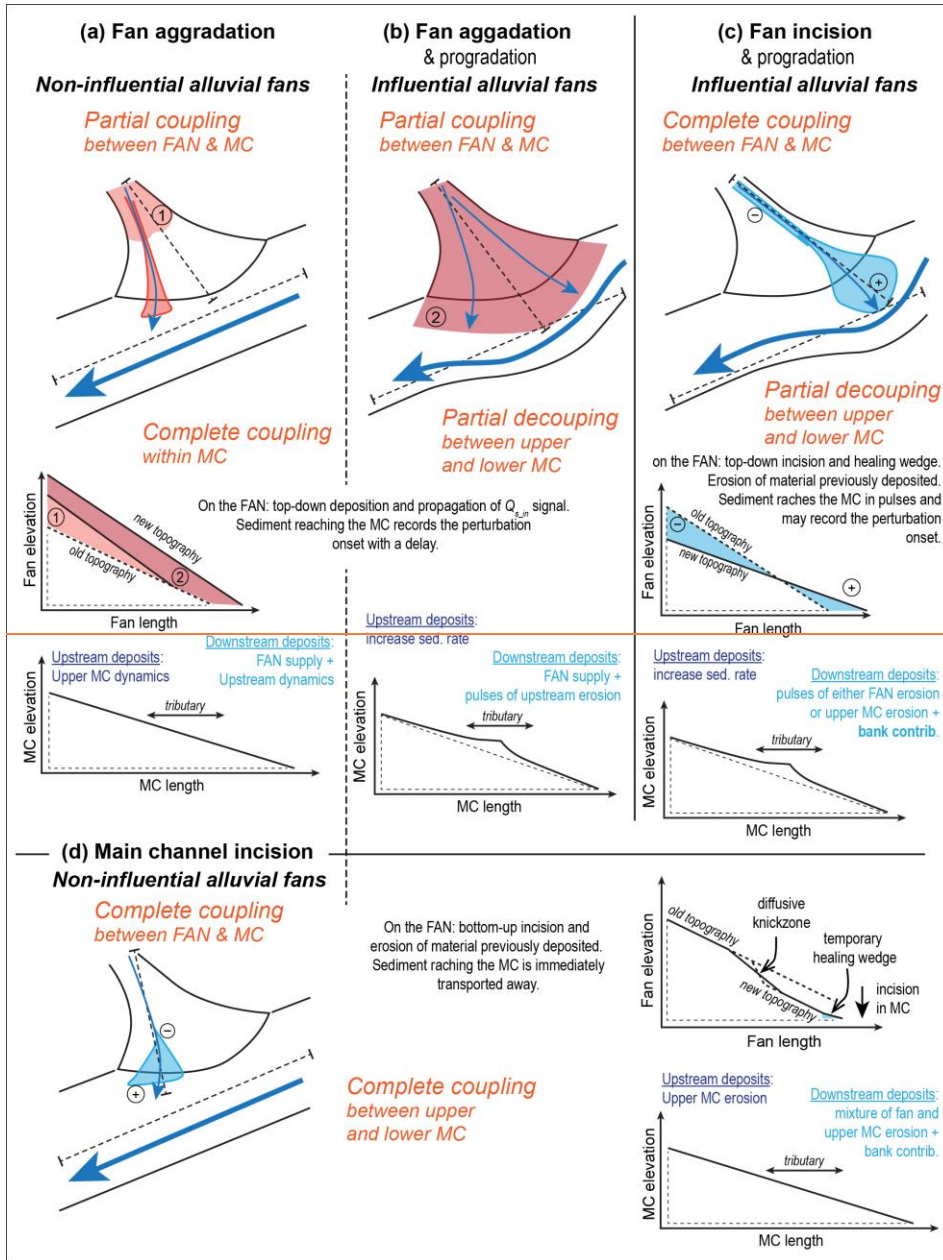
712 5.3.1. Aggrading and incising fans

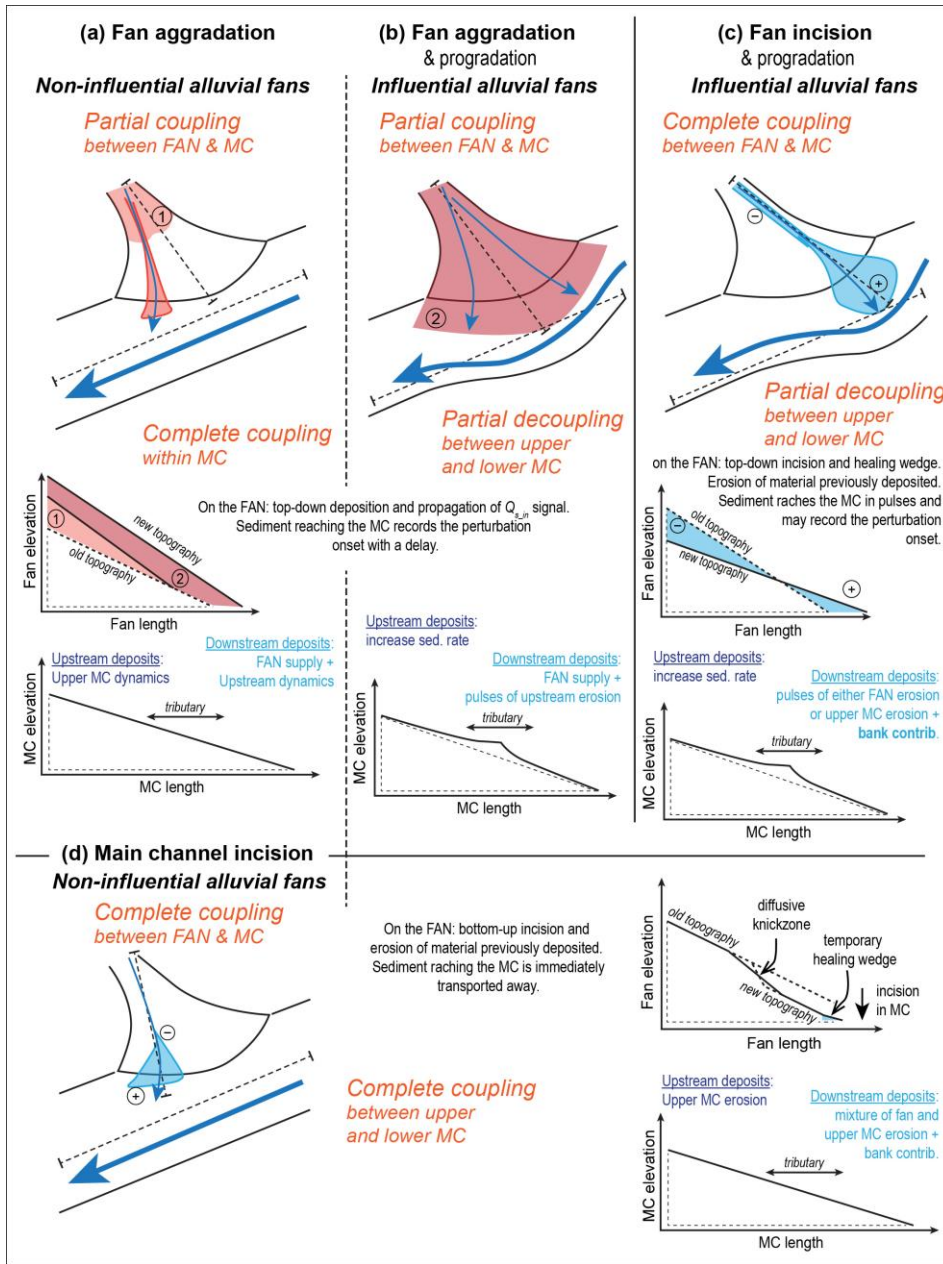
- 713 1. If the tributary has perennial water discharge, a *partial coupling* between the tributary
714 and the main channel is possible. Also, during fan aggradation, when most of the
715 sediment is deposited and stored within the fan (e.g., Fig. 40b, S4b), a portion of the Q_{s_in}
716 reaches the main channel in proportion to the transport capacity of the tributary channel
717 (Fig. 42a10a and b). The partial coupling between the fan and the main channel allows
718 for a *complete coupling* between the upstream and downstream sections of the main river
719 (Fig. 40bS4b – 300-390 min, and S3bS5b in the Supp. Material). As such, during fan
720 aggradation, the main channel behaves as a single connected segment, and the lower
721 section receives sediment in proportion to the transport capacity of the main and tributary
722 channels. The material supplied by the tributary to the main channel is dominated by the
723 tributary's Q_{s_in} with little remobilization of previously deposited material.
- 724 2. During fan incision, large volumes of sediment are eroded from the fan and transported
725 into the main channel as healing wedges, allowing the fan to ~~prograde~~prograde into the
726 main channel (Fig. 40eS4c and 42e10c). This process creates a *complete coupling*
727 between the tributary and the main channel (Fig. 9e8c and d), with the material supplied
728 by the tributary mostly dominated by sediment previously deposited within the fan.
- 729 3. During times of fan progradation, the fan creates an obstacle to the transfer of sediment
730 down the main channel, creating a *partial decoupling* between upstream and downstream
731 sections of the main channel (Fig. 9-8, S4b and c, and 10b and c, and 12b and e). As a
732 consequence, the sediment carried by the main channel is trapped above the tributary
733 junction and thus will be missing from downstream sedimentary deposits. However, the
734 upstream section of the main channel may be periodically subject to incision (e.g., Fig.
735 40bS4b and c), moving mobilized sediment from the upper to the lower section.
736 Accordingly, if progradation of the fan is ~~due to~~caused by prolonged fan aggradation, the
737 downstream section will receive the Q_{s_in} from the fan, plus pulses of sediment eroded
738 from the upstream section of the main channel. Conversely, if progradation is due to
739 incision of the tributary and mobilization of additional fan sediment, the downstream

740 section will receive pulses of erosion from either the fan or the upstream section of the
741 main channel, plus the contribution of bank erosion.

742 In summary, downstream fluvial deposits record the competition between the main
743 channel and the tributary: the alluvial fan pushes the main channel towards the opposite side
744 of the valley to adjust its length, whereas the main channel tries to maintain a straight course
745 by removing the material deposited from the fan. If the main channel dominates, it cuts the
746 fan toe and permits sediment from upstream of the junction to be more easily moved
747 downstream. If the tributary dominates, the main channel will be displaced and the transfer of
748 sediment through the junction will be disrupted. An autogenic alternation of these two
749 situations is possible, whereby fan-toe cutting may trigger fan incision and progradation,
750 increasing the influence of the fan on the main channel. The composition of the sediment
751 downstream thus reflects the competition between main channel and alluvial fan, with
752 contributions from both sub-catchments. In addition, bank erosion may make important
753 contributions to sediment supply and transport, particularly during periods of fan incision
754 (Fig. S6S8 in the Supp. Material). From these results, we therefore distinguish between: 1)
755 *Influential alluvial fans*, which have a strong impact on the geometry and sediment-transfer
756 dynamics of the main channel, and 2) *Non-influential alluvial fans*, which do not
757 substantially alter the geometry or sediment-transfer dynamics of the main channel.

758





761 Figure 4210. Conceptual framework for the coupling conditions of an alluvial-fan/main-channel
762 (MC) system under different environmental forcings. For *aggrading and incising alluvial fans*
763 (upper panels), the fan-main channel connectivity depends on the dynamics acting in the alluvial
764 fan, being partially coupled during fan aggradation and totally coupled during fan incision. For
765 *incising main rivers* (lower panel) the fan and main channel are fully coupled. As well, *non-*
766 *influential alluvial fans* (left and lower panels) favors a complete coupling within the main
767 channel, whereas *influential alluvial fans* (middle and right upper panels) may favor a partial
768 decoupling between upstream and downstream sections of the main river. Each one of the four
769 settings presented here brings its own sedimentary signature, different responses to perturbations,
770 and dynamics of signal propagation which may be recorded into the fluvial deposits.

771

772 5.3.2. *Incising main channel*

- 773 1. Lowering of the main-channel bed triggers incision into the alluvial fan, thereby
774 promoting a *complete coupling* between the fan and the main channel (Fig. 4210d, and
775 S5S7 in the Supp. Material). The sediment supplied by the tributary is mainly composed
776 of material previously deposited within the fan.
- 777 2. An increase in main-channel water discharge increases the transport capacity of the
778 mainstem so that it persistently “wins” the competition with the alluvial fan. In this case,
779 despite the incision triggered in the alluvial fan, which increases the sediment supplied by
780 the tributary, the main channel efficiently removes the additional sediment load, thereby
781 reducing the influence of the alluvial fan on downstream sediment transport within the
782 main channel (Fig. S5 S7 in the Supp. Material). The consequence is a *complete coupling*
783 between the upstream and downstream sections of the main channel (Fig. 4210d). The
784 sediment reaching the lower section is a mixture of eroded material from the main
785 channel, within the fan, and along the banks.

786 5.4. Limitations of the experiments and implications for field studies

787 Physical experiments have the advantage of simulating many of the complexities of natural
788 systems in a simplified setting (Paola et al., 2009). Because of the simplifications, however, a
789 number of limitations arise when attempting to compare experimental results to natural
790 environments. One limitation of our study concerns the small number of experiments that we
791 have performed compared to the full variability of natural river systems and the lack of repetition
792 of experiments. This limitation prevents us, for example, from fully distinguishing significant
793 trends in sediment mobility from stochastic or autogenic processes that are inherent of alluvial

794 systems. In Section 2.2, we described how fan-toe cutting may create the same response in the
795 tributary as incision along the main channel. However, we are not able to quantify the relative
796 contribution of these two processes on the changes occurring in the tributary. One way to
797 distinguish between fan-toe cutting and main-channel incision is to study the whole fluvial
798 system, thus including all tributaries: Main channel variations will affect all tributaries with a
799 timing that is diachronous in the direction of the change (Mather et al., 2017 and references
800 therein). Fan-toe cutting, on the other hand, will be specific of single tributaries with “random”
801 timings.

802 Another limitation of our experiments relates to the *scaling*. Our experiments were not scaled
803 to any particular environment. Instead we used the principle of *similarity of processes* as
804 suggested by Hooke (1968). However, the use of a single grain size for both the tributary and the
805 main channel prevents us from analyzing geomorphic changes that are associated to the input of
806 a coarser grain size from a tributary or to the thinning of sediment in the main channel upstream
807 of the fan. In this regard, we point again to the work of Ferguson et al. (2006) which, by
808 analyzing the effects of grain-size variations on channel slope, may represent a good complement
809 to our analyses. Finally, the patterns highlighted by our experiments are partially dictated by the
810 choices made in setting the values of Q_w and $Q_{s, in}$, and by the timing and the magnitude of the
811 imposed perturbations.

812 Despite these shortcomings, the analysis presented here provides insights into how channels
813 respond to changes in water and sediment discharge at confluence zones, and how sediment
814 moves through branched fluvial systems. In particular, the dynamics that govern the movement
815 of sediment can have important repercussions for field studies, particularly for interpretations of
816 alluvial-channel long profiles, dating of material within stratigraphic sequences, and for
817 interpretations of their geochemical composition (e.g., [Tofelde et al., 2019](#), and references
818 therein). Additionally, by partially decoupling the upper and lower sections of the main channel,
819 fan progradation may lead to pulses of sediment movement from the upper to the lower sections
820 of the main channel, therefore disrupting environmental signals that could be transmitted
821 downstream (e.g., Simpson and Castellort, 2012). Indeed, the stratigraphy of the downstream
822 section of the main channel may record periods of high sedimentation rates, erroneously pointing

823 to periods of high sediment supply, when in reality the fast accumulation may be related to a
824 pulse of sediment being eroded from the upstream section of the main channel.

825 These complexities highlight the need for further research on these topics and the importance
826 of studying the coupled tributary-main channel system to fully understand the dynamics acting in
827 the river network and correctly interpret both geochemical and stratigraphic signals.

828 6. Conclusion

829 We performed six experiments to analyze the interactions of a tributary–main-channel
830 system when a tributary produces an alluvial fan. We found that differing degrees of coupling
831 may be responsible for substantial changes in the geometry of the main channel and the sediment
832 transfer dynamics of the system. In general, we found that the channel geometry (i.e., channel
833 slope and valley width) adjusts to changes in sediment and water discharge in accordance with
834 theoretical models (e.g., Ferguson and Hoey, 2008; Parker et al., 1998; Whipple et al., 1998;
835 Wickert and Schildgen, 2019). Additionally, by analyzing the effects of the tributary-main
836 channel interactions on the downstream delivery of sediment, we have shown that the fluvial
837 deposits within the main channel above and below the tributary junction may record
838 perturbations to the environmental conditions that govern the fluvial system.

839 Our main results can be summarized as follows (Fig. 4210):

840 (1) Fan aggradation leads to a partial coupling between the fan and the main channel, which
841 permits a complete coupling between the main-channel reaches upstream and downstream of the
842 tributary junction. As such, the provenance of downstream sediment reflects the dynamics of
843 both sub-catchments (e.g., tributary and main river), and remobilized material from older
844 deposits will be minimal.

845 (2) Fan incision favors a complete coupling between the fan and the main channel, and
846 remobilizes material previously stored in the fan.

847 (3) Fan progradation (either during prolonged aggradation or fan incision) strongly
848 influences the main channel. As a result, the connectivity of the main river across the tributary
849 junction is reduced and the deposits of the fluvial system above and below the junction may
850 record different processes.

851 (4) Incision along the main channel triggers incision in the alluvial fan that, despite an
852 increased sediment supply to the main river, reduces its influence on the dynamics of the main
853 channel. The result is a fully connected fluvial system in which the deposits record sediment-
854 transfer dynamics and the interactions between both the alluvial fan and the main river, including
855 a large component of material remobilized from older deposits.

856 The theoretical framework proposed in this study aims to illustrate the dynamics acting
857 within a tributary junction, ~~which is an ubiquitous phenomenon across many environments.~~ It
858 provides a first-order analysis of how tributaries affect the sediment delivered to the main
859 channels, and of how sediment is moved through the system under different environmental
860 forcing conditions. ~~With this information we hope to provide a better understanding of the~~
861 ~~composition~~ The (dis)connectivity within the fluvial system has important consequences for the
862 stratigraphy and architecture of ~~fluvial~~ depositional sinks, as it may be responsible for the
863 continuity of the sedimentary deposits found at confluence zones, which is record or for the
864 disruption of the environmental signals carried through the main channel (Simpson and
865 Castelltort, 2012). Our findings may be used to improve the understanding of the interactions
866 between tributaries and main channels, providing essential information for a correct
867 reconstruction of the climatic or tectonic histories of a basin.

868 **Data availability**

869 Data will be made available [through the Sediment Experimentalists Network Project Space to](#)
870 [the SEAD Internal Repository](#).

871 **Video supplement**

872 Time-lapse video of the experiment will be uploaded.

873 **Supplement**

874 Supplement tables and figures can be found in the supplementary document.

875 **Author contributions**

876 SS, ST, and ADW designed and built the experimental setup. SS and ST performed the
877 experiments. SS analyzed the data with the help of ST, ADW and AB. All authors discussed the
878 data, designed the manuscript, and commented on it. SS designed the artwork.

879

880 **Competing interests**

881 The authors declare that they have no conflict of interest.

882

883 **Acknowledgments**

884 We thank Ben Erickson, Richard Christopher, Chris Ellis, Jim Mullin, and Eric Steen for
885 their help in building the experimental setup and installing equipment. We are also thankful to
886 Jean-Louis Grimaud and Chris Paola for fruitful discussions and suggestions.

887

888 **Financial support**

889 This research has been supported by the Deutsche Forschungsgemeinschaft (grant no. SCHI
890 1241/1-1 and grant no. SA 3360/2-1), the Alexander von Humboldt-Stiftung (grant no. ITA
891 1154030 STP), and the University of Minnesota.

892

893 **References**

894 Allen, P. A.: From landscapes into geological history, *Nature*, 451, 274–276,
895 <https://doi.org/10.1038/nature06586>, 2008.
896
897 Armitage, J. J., Duller, R. A., Whittaker, A. C., and Allen, P. A.: Transformation of tectonic
898 and climatic signals from source to sedimentary archive, *Nat. Geosci.*, 4, 231–235, 2011.
899
900 Belmont, P., Gran, K.B., Schottler, S.P., Wilcock, P.R., Day, S.S., Jennings, C., Lauer, J.W.,
901 Viparelli, E., Willenbring, J.K., Engstrom, D.R., and Parker, G.: Large Shift in Source of Fine
902 Sediment in the Upper Mississippi River. *Environmental Science and Technology*, 45, 8804–
903 8810, 2011.
904
905 Benda, L.: Confluence environments at the scale of river networks. In: *River Confluences,*
906 *Tributaries and the Fluvial Network* © John Wiley & Sons, Ltd. ISBN: 978-0-470-02672-4,
907 2008.
908
909 Benda, L., Miller, D., Bigelow, P., and Andras, K.: Effects of post-wildfire erosion on
910 channel environments, *Boise River, Idaho. Forest Ecology and Management*, v. 178, 105–119,
911 doi:10.1016/S0378-1127(03)00056-2, 2003.
912
913 Benda, L., Leroy Poff, N., Miller, D., Dunne, T., Reeves, G., Pess, G., and Pollock, M.: The
914 Network Dynamics Hypothesis: How Channel Networks Structure Riverine Habitats.
915 *BioScience*, v. 54(5), 413-427, 2004a.
916
917 Benda, L., Andras, K., Miller, D., and Bigelow, P.: Confluence effects in rivers: Interactions
918 of basin scale, network geometry, and disturbance regime. *Water Resources Research*, 40,
919 W05402, doi:10.1029/2003WR002583, 2004b.
920
921 Best, J.L.: The morphology of river channel confluences. *Progress in Physical Geography:*
922 *Earth and Environment*, v. 10(2), 157-174, <https://doi.org/10.1177/030913338601000201>, 1986.
923
924 Best, J.L.: Sediment transport and bed morphology at river channel confluences.
925 *Sedimentology*, 35,481-498, 1988.
926
927 Best, J.L., and Rhoads B.L.: Sediment transport, bed morphology and the sedimentology of
928 river channel
929 Confluences. In: *River Confluences, Tributaries and the Fluvial Network* © John Wiley &
930 Sons, Ltd. ISBN: 978-0-470-02672-4, 2008.
931
932 Bierman, P. and Steig, E. J.: Estimating rates of denudation using cosmogenic isotope
933 abundances in sediment, *Earth Surf. Proc. Land.*, 21, 125–139,
934 [https://doi.org/10.1002/\(SICI\)1096-9837\(199602\)21:2<125::AID-ESP511>3.0.CO;2-8](https://doi.org/10.1002/(SICI)1096-9837(199602)21:2<125::AID-ESP511>3.0.CO;2-8), 1996.
935
936 Brown, E. T., Stallard, R. F., Larsen, M. C., Raisbeck, G. M., and Yiou, F.: Denudation rates
937 determined from the accumulation of in situ-produced ¹⁰Be in the Luquillo Experimental Forest,
938 Puerto Rico, *Earth Planet. Sc. Lett.*, 129, 193–202, [https://doi.org/10.1016/0012-](https://doi.org/10.1016/0012-821X(94)00249-X)
939 [821X\(94\)00249-X](https://doi.org/10.1016/0012-821X(94)00249-X), 1995.

940
941 Bryant M., Falk P., and Paola C.: Experimental study of avulsion frequency and rate of
942 deposition. *Geology*; v. 23; no. 4; 365–368, 1995.
943
944 Bufe, A., Turowski, J.M., Burbank, D.W., Paola, C., Wickert, A.D., and Tofelde, S.:
945 Controls on the lateral channel migration rate of braided channel systems in coarse non-cohesive
946 sediment. *Earth Surface Processes and Landforms*, <https://doi.org/10.1002/esp.4710>, 2019.
947
948 Bull W.B.: Threshold of critical power in streams. *Geological Society of America Bulletin*,
949 Part I, v. 90, 453-464, 1979.
950
951 Castellort S., and Van Den Driessche J.: How plausible are high-frequency sediment
952 supply-driven cycles in the stratigraphic record? *Sedimentary Geology*, v. 157, 3–13;
953 doi:10.1016/S0037-0738(03)00066-6, 2003.
954
955 Clarke L. E., Quine T.A., and Nicholas A.P.: Sediment Dynamics in Changing
956 Environments (Proceedings of a symposium held in Christchurch, New Zealand, December
957 2008). IAHS Publ. 325, 2008.
958
959 Clarke L. E., Quine T.A., and Nicholas A.P.: An experimental investigation of autogenic
960 behaviour during alluvial fan evolution. *Geomorphology*, v. 115, 278–285;
961 doi:10.1016/j.geomorph.2009.06.033, 2010.
962
963 Cohen, T.J., and Brierley, G.J.: Channel instability in a forested catchment: a case study
964 from Jones Creek, East Gippsland, Australia. *Geomorphology*, 32, 109–128, 2000.
965
966 D'Arcy, M., Roda-Boluda, D.C., Whittaker, A.C.: Glacial-interglacial climate changes
967 recorded by debris flow fan deposits, Owens Valley, California. *Quaternary Science Reviews*,
968 169, 288-311, 2017.
969
970 Dingle, E. H., Attal, M., and Sinclair, H. D.: Abrasion-set limits on Himalayan gravel flux,
971 *Nature*, 544, 471–474, 5 <https://doi.org/10.1038/nature22039>, 2017.
972
973 De Haas T., Van den Berg W., Braat L., and Kleinans M.G.: Autogenic avulsion,
974 channelization and backfilling dynamics of debris-flow fans. *Sedimentology*, v. 63, 1596–1619.
975 Doi; 10.1111/sed.12275, 2016.
976
977 Densmore A.L., Allen P.A., and Simpson G.: Development and response of a coupled
978 catchment fan system under changing tectonic and climatic forcing. *J. Geophys. Res.*, 112,
979 F01002, doi:10.1029/2006JF000474, 2007
980
981 Faulkner, D.J., Larson, P.H., Jol, H.M., Running, G.L., Loope, H.M., and Goble, R.J.:
982 Autogenic incision and terrace formation resulting from abrupt late-glacial base-level fall, lower
983 Chippewa River, Wisconsin, USA. *Geomorphology*, v. 266, 75–95,
984 <http://dx.doi.org/10.1016/j.geomorph.2016.04.016>, 2016.
985

986 Ferguson, R.I., Cudden, J.R., Hoey, T.B., and Rice, S.P.: River system discontinuities due to
987 lateral inputs: generic styles and controls. *Earth Surf. Process. Landforms*, v. 31, 1149–1166, doi:
988 10.1002/esp.1309, 2006.

989
990 Ferguson, R.I., and Hoey, T.: Effects of tributaries on main-channel geomorphology. In:
991 *River Confluences, Tributaries and the Fluvial Network* © John Wiley & Sons, Ltd. ISBN: 978-
992 0-470-02672-4, 2008.

993
994 Gao L., Wang X., Yi S., Vandenberghe J., Gibling M.R., and Lu H.: Episodic Sedimentary
995 Evolution of an Alluvial Fan (Huangshui Catchment, NE Tibetan Plateau). *Quaternary*, v. 1(16);
996 doi:10.3390/quat1020016, 2018.

997
998 Germanoski, D., Ritter, D.F.: Tributary response to local base level lowering below a dam.
999 *Regulated rivers: research and management*, v. 2, 11-24, 1988.

1000
1001 Gilbert, G. K.: Report on the Geology of the Henry Mountains, US Gov. Print. Off.,
1002 Washington, D.C., USA, <https://doi.org/10.3133/70038096>, 1877.

1003
1004 Giles P.T., Whitehouse B.M., and Karymbalis E.: Interactions between alluvial fans and
1005 axial rivers in
1006 Yukon, Canada and Alaska, USA. From: Ventra, D. & Clarke, L. E. (eds) *Geology and
1007 Geomorphology of Alluvial and Fluvial Fans: Terrestrial and Planetary Perspectives*. Geological
1008 Society, London, Special Publications, v. 440; <http://doi.org/10.1144/SP440.3>, 2016.

1009
1010 Gippel, C.: Changes in stream channel morphology at tributary junctions, Lower Hunter
1011 Valley,
1012 New South Wales. *Australian Geographical Studies*, v. 23, 291-307, 1985.

1013
1014 Grant, G.E., and Swanson, F.J.: Morphology and Processes of Valley Floors in Mountain
1015 Streams,
1016 Western Cascades, Oregon. *Natural and Anthropogenic Influence in Fluvial
1017 Geomorphology*, Geophysical Monograph, 89, 1995.

1018
1019 Granger, D. E., Kirchner, J. W., and Finkel, R.: Spatially averaged long-term erosion rates
1020 measured from in situ-produced cosmogenic nuclides in alluvial sediment, *J. Geol.*, 104, 249–
1021 257, 1996.

1022
1023 Heine, R.A., and Lant, C.L.: Spatial and Temporal Patterns of Stream Channel Incision in
1024 the Loess Region of the Missouri River, *Annals of the Association of American Geographers*,
1025 99(2), 231-253, DOI: 10.1080/00045600802685903, 2009.

1026
1027 Hamilton P.B., Strom K., and Hoyal D.C.J.D.: Autogenic incision-backfilling cycles and
1028 lobe formation during the growth of alluvial fans with supercritical distributaries.
1029 *Sedimentology*, v. 60, 1498–1525; doi: 10.1111/sed.12046, 2013.

1030

1031 Hooke R.L.: Model Geology: Prototype and Laboratory Streams: Discussion. Geological
1032 Society of America Bulletin, v. 79, 391-394, 1968.

1033

1034 Hooke R.L., and Rohrer W.L.: Geometry of alluvial fans: effect of discharge and sediment
1035 size. Earth Surface Processes, v. 4, 147-166, 1979.

1036

1037 Kim W., and Jerolmack D.J.: The Pulse of Calm Fan Deltas. The Journal of Geology, 11(4),
1038 315-330; <http://dx.doi.org/10.1086/588830>, 2008.

1039

1040 Lane, E. W.: Importance of fluvial morphology in hydraulic engineering, Proceedings of the
1041 American Society of Civil Engineers, 81, 1–17, 1955.

1042

1043 Larson P.H., Dorn R.I., Faulkner D.J., and Friend d.A.: Toe-cut terraces: A review and
1044 proposed criteria to differentiate from traditional fluvial terraces. Progress in Physical
1045 Geography, v. 39(4), 417–439, 2015.

1046

1047 Leeder M.R., and Mack G.H.: Lateral erosion (“toe-cutting”) of alluvial fans by axial rivers:
1048 implications for basin analysis and architecture. Journal of the Geological Society, London, v.
1049 158, 885-893, 2001.

1050

1051 Leopold, L.B., and Maddock, T. Jr.: The Hydraulic Geometry of Stream Channels and Some
1052 Physiographic Implications. Geological survey professional paper 252, 1953.

1053

1054 Lupker, M., Blard, P., Lavé, J., France-Lanord, C., Leanni, L., Puchol, N., Charreau, J., and
1055 Bourlès, D.: ¹⁰Be-derived Himalayan denudation rates and sediment budgets in the Ganga basin.
1056 Earth and Planetary Science Letters, 333–334, 146–156, doi:
1057 <http://dx.doi.org/10.1016/j.epsl.2012.04.020>, 2012.

1058

1059 Mackin J.H.: Concept of the graded river. Bulletin of the Geological Society of America, v.
1060 69, 463-512, 1948.

1061

1062 Mather A.E., Stokes M., and Whitfield E.: River terraces and alluvial fans: The case for an
1063 integrated Quaternary fluvial archive. Quaternary Science Reviews, v. 166, 74-90;
1064 <http://dx.doi.org/10.1016/j.quascirev.2016.09.022>; 2017.

1065

1066 Meyer-Peter, E. and Müller, R.: Formulas for Bed-Load Transport, in: 2nd Meeting of the
1067 International Association for Hydraulic Structures Research, 7–9 June 1948, Stockholm,
1068 Sweden, International
1069 Association for Hydraulic Structures Research, 39–64, 1948.

1070

1071 Miller, J.P.: High Mountain Streams: Effects of Geology on Channel Characteristics and
1072 Bed Material. State bureau of mines and mineral resources New Mexico institute of mining and
1073 technology Socorro, New Mexico. Memoir 4, 1958.

1074

1075 Mouchéné, M., van der Beek, P., Carretier, S., and Mouthereau, F.: Autogenic versus
1076 allogenic controls on the evolution of a coupled fluvial megafan–mountainous catchment system:

1077 numerical modelling and comparison with the Lannemezan megafan system (northern Pyrenees,
1078 France). *Earth Surf. Dynam.*, 5, 125–143, doi:10.5194/esurf-5-125-2017, 2017.
1079
1080 Nicholas, A.P., Quine, T.A.: Modeling alluvial landform change in the absence of external
1081 environmental forcing. *Geology*, v. 35(6), 527–530; doi: 10.1130/G23377A.1, 2007.
1082
1083 Nicholas, A. P., Clarke L., and Quine T. A.: A numerical modelling and experimental study
1084 of flow width dynamics on alluvial fans. *Earth Surf. Process. Landforms* 34, 1985–1993;
1085 DOI: 10.1002/esp.1839;, 2009.
1086
1087 Paola, C., Straub, K., Mohrig, D., and Reinhardt L.: The “unreasonable effectiveness” of
1088 stratigraphic and geomorphic experiments. *Earth-Science Reviews*, v. 97(1–4), 1-43,
1089 <https://doi.org/10.1016/j.earscirev.2009.05.003>, 2009.
1090
1091 Parker, G.: Hydraulic geometry of active gravel rivers, *J. Hydraul. Div.*, 105, 1185–1201,
1092 1978.
1093
1094 Parker, G.: Progress in the modeling of alluvial fans, *Journal of Hydraulic Research*, 37(6),
1095 805-825, <http://dx.doi.org/10.1080/00221689909498513>, 1999.
1096
1097 Parker, G. Paola, C., Whipple, K.X., and Mohrig, D.: Alluvial fans formed by channelized
1098 fluvial
1099 And sheet flow. I: Theory. *Journal of Hydraulic Engineering*, v. 124(10), 1998.
1100
1101 Pepin, E., Carretier, S., and Herail, G.: Erosion dynamics modelling in a coupled catchment–
1102 fan system with constant external forcing. *Geomorphology*, v. 122, 78–90,
1103 doi:10.1016/j.geomorph.2010.04.029, 2010.
1104
1105 Reitz, M.D., Jerolmack, D.J., and Swenson J.B.: Flooding and flow path selection on
1106 alluvial fans and deltas. *Geophysical Research Letters*, v. 37, L06401,
1107 doi:10.1029/2009GL041985, 2010.
1108
1109 Reitz, M.D., and Jerolmack, D.J.: Experimental alluvial fan evolution: Channel dynamics,
1110 slope controls, and shoreline growth. *Geophysical Research Letters*, v. 117, F02021,
1111 doi:10.1029/2011JF002261, 2012.
1112
1113 Rice, S.P., and Church, M.: Longitudinal profiles in simple alluvial systems. *Water*
1114 *Resources Research*, v. 37(2), 417-426, 2001.
1115
1116 Rice, S.P., Kiffney, P., Greene, C., and Pess, G.R.: The ecological importance of tributaries
1117 and confluences. In: *River Confluences, Tributaries and the Fluvial Network* © John Wiley &
1118 Sons, Ltd. ISBN: 978-0-470-02672-4, 2008.
1119
1120 Ritter, J.B., Miller, J.R., Enzel, Y., and Wells, S.G.: Reconciling the roles of tectonism and
1121 climate in Quaternary alluvial fan evolution. *Geology*, v. 23(3), 245–248, 1995.
1122

1123 Rohais, S., Bonnet, S., and Eschard, R.: Sedimentary record of tectonic and climatic
1124 erosional perturbations in an experimental coupled catchment-fan system. *Basin Research*, v. 24,
1125 198–212, doi: 10.1111/j.1365-2117.2011.00520.x, 2012.
1126
1127 Savi, S., Norton, K. P., Picotti, V., Akçar, N., Delunel, R., Brardinoni, F., Kubik, P., and
1128 Schlunegger, F.: Quantifying sediment supply at the end of the last glaciation: Dynamic
1129 reconstruction of an alpine debris-flow fan, *GSA Bull.*, 126, 773–790,
1130 <https://doi.org/10.1130/B30849.1>, 2014.
1131
1132 Savi, S., Schildgen T. F., Tofelde S., Wittmann H., Scherler D., Mey J., Alonso R. N., and
1133 Strecker M. R.: Climatic controls on debris-flow activity and sediment aggradation: The Del
1134 Medio fan, NW Argentina, *J. Geophys. Res. Earth Surf.*, 121, 2424–2445,
1135 doi:10.1002/2016JF003912, 2016.
1136
1137 Schildgen, T. F., Robinson, R. A. J., Savi, S., Phillips, W. M., Spencer, J. Q. G., Bookhagen,
1138 B., Scherler, D., Tofelde, S., Alonso, R. N., Kubik, P. W., Binnie, S. A., and Strecker, M. R.:
1139 Landscape response to late Pleistocene climate change in NW Argentina: Sediment flux
1140 modulated by basin geometry and connectivity, *J. Geophys. Res.-Earth*, 121, 392–414,
1141 <https://doi.org/10.1002/2015JF003607>, 2016.
1142
1143 Schumm, S. A.: Geomorphic thresholds and complex response of drainage systems, *Fluv.*
1144 *Geomorphol.*, 6, 69–85, 1973.
1145
1146 Schumm, S. A. and Parker, R. S.: Implication of complex response of drainage systems for
1147 Quaternary alluvial stratigraphy, *Nat. Phys. Sci.*, 243, 99–100, 1973.
1148
1149 Schwanghart, W. and Scherler, D.: Short Communication: TopoToolbox 2 – MATLAB-
1150 based software for topographic analysis and modeling in Earth surface sciences, *Earth Surf.*
1151 *Dynam.*, 2, 1-7, <https://doi.org/10.5194/esurf-2-1-2014>, 2014.
1152
1153 Simon, A., and Rinaldi, M.: Channel instability in the loess area of the midwestern United
1154 States. *Journal of the American Water Resources Association*, v. 36(1), Paper No. 99012, 2000.
1155
1156 Straub, K.M., Paola, C., Mohrig, D., Wolinsky, M.A., and George, T.: Compensational
1157 stacking of channelized sedimentary deposits. *Journal of Sedimentary Research*, v. 79, 673–688,
1158 doi: 10.2110/jsr.2009.070, 2009.
1159
1160 Tofelde, S., Savi, S., Wickert, A. D., Bufe, A., and Schildgen, T. F.: Alluvial channel
1161 response to environmental perturbations: fill-terrace formation and sediment-signal disruption,
1162 *Earth Surf. Dynam.*, 7, 609-631, <https://doi.org/10.5194/esurf-7-609-2019>, 2019.
1163
1164 Van den Berg van Saparoea, A.P. H., and Postma, G.: Control of climate change on the yield
1165 of river systems, *Recent Adv. Model. Siliciclastic Shallow-Marine Stratigr. SEPM Spec. Publ.*,
1166 90, 15–
1167 33, 2008.
1168

1169 Van Dijk, M., Postma, G., and Kleinhans, M.G.: Autocyclic behaviour of fan deltas: an
1170 analogue experimental study. *Sedimentology*, v. 56, 1569–1589, doi: 10.1111/j.1365-
1171 3091.2008.01047.x, 2009.
1172
1173 Van Dijk, M., Kleinhans, M.G., Postma, G., and Kraal, E.: Contrasting morphodynamics in
1174 alluvial fans and fan deltas: effect of the downstream boundary. *Sedimentology*, v. 59, 2125–
1175 2145 doi: 10.1111/j.1365-3091.2012.01337.x, 2012.
1176
1177 Von Blanckenburg, F.: The control mechanisms of erosion and weathering at basin scale
1178 from cosmogenic nuclides in river sediment. *Earth and Planetary Science Letters*, v. 237, 462–
1179 479, 2005.
1180
1181 Whipple, K.X., Parker, G. Paola, C., and Mohrig, D.: Channel Dynamics, Sediment
1182 Transport, and the Slope of Alluvial Fans: Experimental Study. *The Journal of Geology*, v. 106,
1183 677–693, 1998.
1184
1185 Whipple, K.X., and Tucker, G.E.: Implications of sediment-flux-dependent river incision
1186 models for landscape evolution. *Journal of Geophysical Research*, 107, B2, 2039, doi:
1187 10.1029/2000JB000044, 2002.
1188
1189 Wickert, A. D. and Schildgen, T. F.: Long-profile evolution of transport-limited gravel-bed
1190 rivers, *Earth Surf. Dynam.*, 7, 17–43, <https://doi.org/10.5194/esurf-7-17-2019>, 2019.
1191
1192 Wittmann, H., and von Blanckenburg, F.: Cosmogenic nuclide budgeting of floodplain
1193 sediment transfer. *Geomorphology*, 109, 246–256, 2009.
1194
1195 Wittmann, H., von Blanckenburg, F., Maurice, L., Guyot, J., Filizola, N., and Kubik, P.W.:
1196 Sediment production and delivery in the Amazon River basin quantified by in situ-produced
1197 cosmogenic nuclides and recent river loads. *GSA Bulletin*, 123 (5-6), 934–950, doi:
1198 <https://doi.org/10.1130/B30317.1>, 2011.
1199